energies

MDPI

Article

Estimates of the Decarbonization Potential of Alternative Fuels for Shipping as a Function of Vessel Type, Cargo, and Voyage

Li Chin Law [1,2,*], Epaminondas Mastorakos [1,3,*] and Stephen Evans [1,3]

[1] Cambridge Centre for Advanced Research and Education in Singapore (CARES), CREATE Tower, 1 Create Way, Singapore 138602, Singapore
[2] School of Chemical Engineering, Engineering Campus, Universiti Sains Malaysia, Nibong Tebal 14300, Penang, Malaysia
[3] Engineering Department, University of Cambridge, Cambridge CB2 1TN, UK
* Correspondence: lcl38@cam.ac.uk or lichin.cares@gmail.com (L.C.L.); em257@eng.cam.ac.uk (E.M.); Tel.: +65-88852052 (L.C.L.)

Abstract: Fuel transition can decarbonize shipping and help meet IMO 2050 goals. In this paper, HFO with CCS, LNG with CCS, bio-methanol, biodiesel, hydrogen, ammonia, and electricity were studied using empirical ship design models from a fleet-level perspective and at the Tank-To-Wake level, to assist operators, technology developers, and policy makers. The cargo attainment rate CAR (i.e., cargo that must be displaced due to the low-C propulsion system), the E_S (i.e., TTW energy needed per ton*n.m.), the C_S (economic cost per ton*n.m.), and the carbon intensity index CII (gCO_2 per ton*n.m.) were calculated so that the potential of the various alternatives can be compared quantitatively as a function of different criteria. The sensitivity of CAR towards ship type, fuel type, cargo type, and voyage distance were investigated. All ship types had similar CAR estimates, which implies that considerations concerning fuel transition apply equally to all ships (cargo, containership, tankers). Cargo type was the most sensitive factor that made a ship either weight or volume critical, indirectly impacting on the CAR of different fuels; for example, a hydrogen ship is weight-critical and has 2.3% higher CAR than the reference HFO ship at 20,000 nm. Voyage distance and fuel type could result in up to 48.51% and 11.75% of CAR reduction. In addition to CAR, the E_S, C_S, and CII for a typical mission were calculated and it was found that HFO and LNG with CCS gave about 20% higher E_S and C_S than HFO, and biodiesel had twice the cost, while ammonia, methanol, and hydrogen had 3–4 times the C_S of HFO and electricity about 20 times, suggesting that decarbonisation of the world's fleet will come at a large cost. As an example of including all factors in an effort to create a normalized scoring system, an equal weight was allocated to each index (CAR, E_S, C_S, and CII). Biodiesel achieved the highest score (80%) and was identified as the alternative with the highest potential for a deep-seagoing containership, followed by ammonia, hydrogen, bio-methanol, and CCS. Electricity has the lowest normalized score of 33%. A total of 100% CAR is achievable by all alternative fuels, but with compromises in voyage distance or with refuelling. For example, a battery containership carrying an equal amount of cargo as an HFO-fuelled containership can only complete 13% of the voyage distance or needs refuelling seven times to complete 10,000 n.m. The results can guide decarbonization strategies at the fleet level and can help optimise emissions as a function of specific missions.

Keywords: ship design; tanker; cargo ship; containership; maritime energy; marine fuel; alternative fuels; decarbonization

Citation: Law, L.C.; Mastorakos, E.; Evans, S. Estimates of the Decarbonization Potential of Alternative Fuels for Shipping as a Function of Vessel Type, Cargo, and Voyage. *Energies* **2022**, *15*, 7468. https://doi.org/10.3390/en15207468

Academic Editors: Theodoros Zannis, Apostolos Pesyridis and Dimitrios Kyritsis

Received: 9 September 2022
Accepted: 7 October 2022
Published: 11 October 2022

1. Introduction

Today, 96% of the bunker fuels used to power ships are made of fossil fuels, making shipping responsible for 2.8% of global GHG emissions or 1036 Mt of CO_2e per annum [1]. As reported in the Fourth IMO Greenhouse Gas Study, GHG shipping emissions will increase by up to 50% to 1500 Mt CO_2 following the rise in seaborne trade activities [1]. Currently, speed reduction and installation of energy saving technologies are the main approaches for shipping decarbonisation. Speed reduction can potentially save up to 34% of energy [2], however, it was demonstrated in recent studies [3] that the classical cubic law for fuel consumption-speed curve only holds near the vessel design speed and that the energy saving was anticipated to be lower. In addition, Berthhelsen et al. [4] suggested that the effect of slow steaming in carbon reduction has been overestimated. Energy saving technologies, for example the Flettner rotor, air cavity lubrication system, flex tunnel and hull vane, were proven effective in energy saving, however, the energy saving is between 10–15% [2]. Hence, these approaches are not sufficient to achieve IMO's 2050 goal and the use of low-carbon alternative fuels and carbon capture appear to be necessary to reach reductions in carbon emissions up to 50%.

The maritime industry has already started to operate vessels with fuels different than the conventional HFO [5], for example LNG and biofuels. Both LNG and biodiesel can be burned in an ICE that gives at least 40% efficiency, and since the conversion of existing vessels to biodiesel and LNG requires minor retrofits, these alternative fuels emerge as an interesting solution for shipowners, at least in the short term. Methanol (denoted for convenience as MeOH in this paper) is another alternative fuel that can be burned easily in an ICE and is stored in the liquid phase, and so MeOH also gets attention. Maersk will reportedly invest USD 1.4 billion on eight ocean-going vessels with capacity to carry 16,000 containers, claimed to be ready to set to sail from early 2024 [6]. Apart from ICE, some vessels may be fitted with higher efficiency propulsion systems such as fuel cells and electrical motors. Battery-based ships and hybrid ships have been commercialized for short trips and small-scale vessels, driven by their higher energy efficiency and robustness of the battery system [7]. Although the fuel cells available in the market may still require optimization, there are a few projects for vessels. In 2014, the HySeas project conducted a commercial study for a hydrogen fuel cell-powered vessel that later integrated PEM fuel cells to a sea-going ferry [8]. Toyota developed a fuel cell system for the world first hydrogen-powered vessel, the Energy Observer [9]. In 2021, Shell in collaboration with Sembcorp Marine Ltd. developed a plan to install PEM fuel cells on an existing Ro-Ro vessel in Singapore [10,11]. This shows that fuel cells are getting increasing attention, with hydrogen and ammonia as the key energy carriers. In addition, installation of onboard CCS to capture CO_2 from vessel's exhaust has also been implemented; for instance, Nordica is the first vessel operated with onboard CCS [12].

Although the above demonstration projects show the practical interest in decarbonisation technologies, there is still need for significant research on the technologies themselves and on system-level studies to determine the optimum solutions for the short or long term. LNG has been suggested as the fuel with the most potential for shipping [13,14]. In 2018, DNV.GL examined the implication of alternative fuels to replace conventional marine fuels and identified LNG, LPG, methanol, and biofuels as the most promising solutions [15], which are capable of meeting the emission limits with cost comparable to oil-fuelled systems with a scrubber [16], DNV.GL also forecasted the demand of LNG to be increased exponentially [17]. Law et al. [18] consistently compared various low-carbon alternatives against HFO and ranked onboard CCS for fossil-fuelled ship and biofuels as the best low-carbon solution, in terms of energy and financial cost, when expressed per Joule of propeller work. Those calculations did not include ship design and operating condition, and therefore the energy, GHG, and financial cost per ton of cargo and distance travelled, which are important ratios in practice, could not be evaluated. However, a fleet-level assessment would be an insightful way to determine alternative fuel potential.

Some fleet-level assessment addressed the impact of fuel transition on cargo attainment. For example, Ref. [19] suggested that a bulk carrier with approximately 82,000 DWT experienced a reduction in cargo capacity with zero carbon fuels. Horvath et al. [20] showed that hydrogen fuel would result in a higher cargo space loss of up to 13.3% for a short-sea vessel, which was contradicting to the 5% cargo loss reported by the International

Council on Clean Transportation [21]. Imhoff et al. showed that ammonia fuel could result in cargo loss between 4–9% [22]. In addition, some studies compared the performance of ships powered by different fuels. Smith et al. [23] concluded that the liquefied H_2 carrier would have to be 1.7 times larger than an LNG carrier by volume, whereas Kim et al. [24] concluded that an ammonia-based ship requires 1.6–2.3 times more volume and 1.4–1.6 times more weight than a conventional HFO-based ship. These studies give some implications on the impact of fuel transition on cargo loss, however, there is lack of consistency possibly due to the different approaches or assumptions in the assessment, which make it difficult to systematically compare the potential of different alternative fuels. In addition, the previous research also neglected the specific characteristics of the ship such as size, deadweight and ship type, which could result in variation in cargo capacity. Hence, more detailed studies still need to be done to cover a wider range of ships, so that the result could reliably reflect the potential of fuel transition. Since the performance of a future decarbonised ship should not be concluded based on the cargo loss only, an assessment from different perspectives, especially energy and cost, should be included, for example the techno-economic assessment of advanced fuel done by Korberg et al which compared the performance of fossil-free ship from energy and cost perspectives [25].

There are many types of ships in operation, which have different size, carry different types of cargo and travel for different distances. The novelty of this research is the inclusion of a wide range of ships by considering four ship design factors, namely fuel type, ship type, cargo type, and voyage distance. Three types of ships are included: a cargo ship, tanker, and containership, hence covering the majority of current vessels. The type of cargo determines the stowage factor (volume per mass), and here the stowage factor was varied from 0.5 m^3/ton to 4 m^3/ton, covering most types of cargo today [26]. Based on the voyage range of all ships derived from AIS [27], the vessels were assessed for voyage distances between 2000 and 20,000 nautical miles. Eight fuel pathways were selected including HFO as reference fuel, HFO with CCS installation, LNG with CCS, bio-MeOH, biodiesel, NG-hydrogen, NG-ammonia, and NG-electricity. These were the top-ranked scenarios with more than 50% of lifecycle carbon reduction as discussed in our previous work [17].

Apart from the broad coverage of ships, the addition of an analysis of the ship performance using various performance indicators (CAR, E_S, C_S, and CII) also make this study useful for various stakeholders in maritime decarbonization. Among all, CAR is the most common performance indicator used in fleet-level assessment to express the cargo loss [20–22], studied the influence of refuelling stops and cargo loss allowance on the CAR [27], whereas E_S and C_S are specific indicators defined in this study to quantify the TTW energy and TTW cost to transport cargo per nautical mile and ship deadweight. CII which is a rating system developed by IMO to measure the CO_2 emission per cargo capacity and nautical mile, which is also included as one of the performance indicators for quantification of the potential of carbon reduction of alternative fuels [28,29]. Usage of these numerical indicators allows a quantitative comparison between ships. By using the same assumption in calculation of the ship performance indicators (per unit of ship deadweight and voyage distance), different ships can be compared consistently. This study demonstrates the variation in CAR for different ships, whereby different ships are designed by varying the design parameters (ship type, cargo type, voyage distance, fuel type) of the ship. The outcome emphasizes the significant of ship type and mission towards the suitability of different alternative fuels to replace HFO. The last part of the study also demonstrates the application of the outcome to justify the design of the ship, so that the ship could be powered by selected alternative fuels. Shipowners and other stakeholders in the maritime industry can use the results and the present methodology to take consistent decisions in fuel transition. Hence, the results obtained from this work are an important step for shipping decarbonization via fuel transition.

In the next section, the research methodology is presented. Section 3 includes the results of exploration of sensitivity of CAR towards ship design factors (Section 3.1). A case study for deep-seagoing containership powered by alternative fuels is presented in

Section 3.2, and another case study for ship propulsion with alternative fuels with upper limits for cargo loss is presented in Section 3.3. Section 4 includes a discussion for the results, while Section 5 summarizes the conclusions from this work.

2. Methods

2.1. Reference Ship and Performance Indices

This paper refines the results of Ref. [17] and performs further estimates of cargo attainment rate, specific energy needed, carbon emitted, and economic cost. In Ref. [17], 22 potential pathways for marine decarbonisation were compared using five quantifiable parameters. Based on the database and ranking of these 22 alternative fuel pathways, 8 top ranked alternative fuels were chosen, covering the most discussed marine fuels including HFO with CCS, LNG with CCS, bio-MeOH, biodiesel, hydrogen, ammonia, and electricity, with HFO without CCS as the reference fuel representing today's fleet. The production pathways and primary energy of these fuels were not prioritized in this study and the Tank-to-Wake (TTW) performance of different type of fuels was instead highlighted. Here, hydrogen and ammonia were assumed to provide propeller work through a fuel cell propulsion system, electricity with battery and electrical motor, and ICE was assumed for the other fuels. Figure 1 summarizes the process workflow. Firstly, ship data for a reference ship, obtained from Marine Optima [30] and Vessel Finder [31], are summarized in Table 1. This vessel was assumed to sail 280 days annually [32], with a sailing speed of 14 knots. Next, ship sizing was carried out using equations published in Practical Ship Design [32] and the method of correlation in Ref. [33]; details are presented in Appendix A. From the ship sizing, the displacement (Δ), ship dimensions (L, B, and T), the gross and net tonnage (GT and NT) were obtained, and then the ship's weight and volume distribution as demonstrated in Figure 2 were calculated.

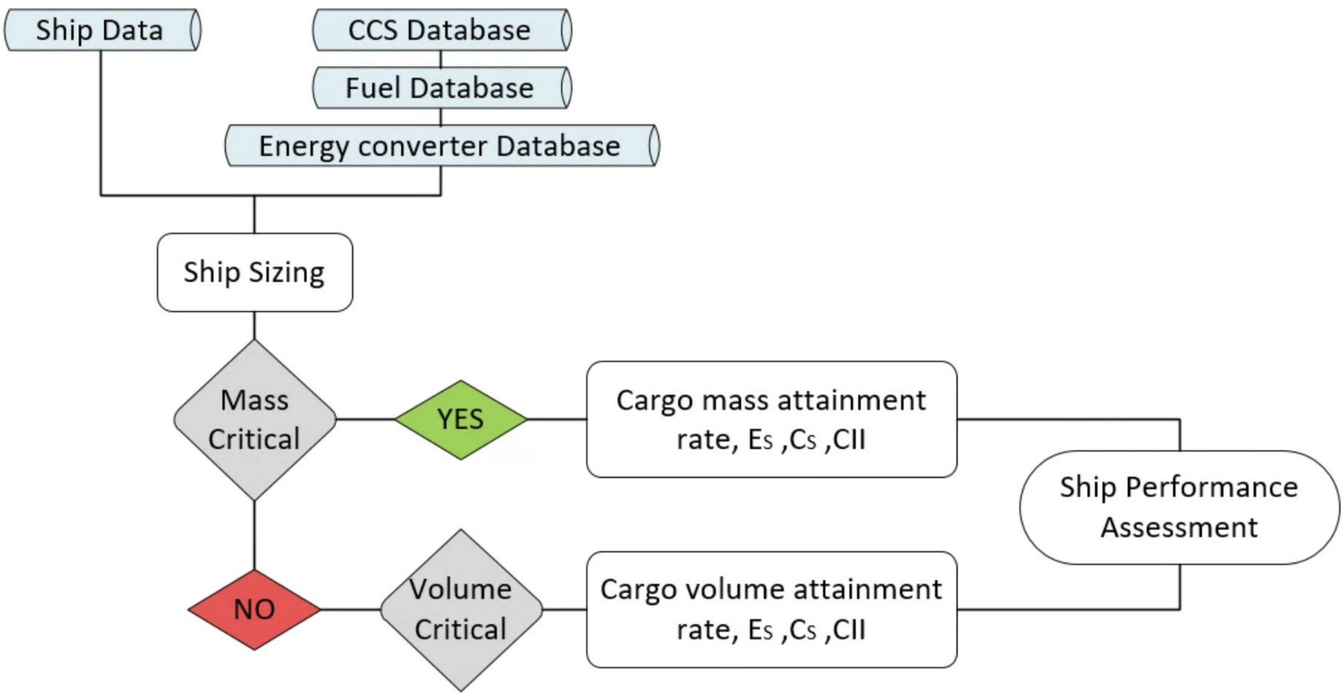

Figure 1. Research process flow diagram.

Table 1. Data of the reference ship (HFO-fuelled containership).

Category	Specification
Ship type	Containership
Fuel type	HFO (no CCS)
Cargo type (stowage factor in m^3/ton)	General cargo (1.25)
Cargo density (kg/m^3)	800
Voyage distance (n.m.)	10,000
Voyage speed (knots)	14
Deadweight capacity (DWT)	156,458
Crew (persons)	25
Engine power (kW)	15,310

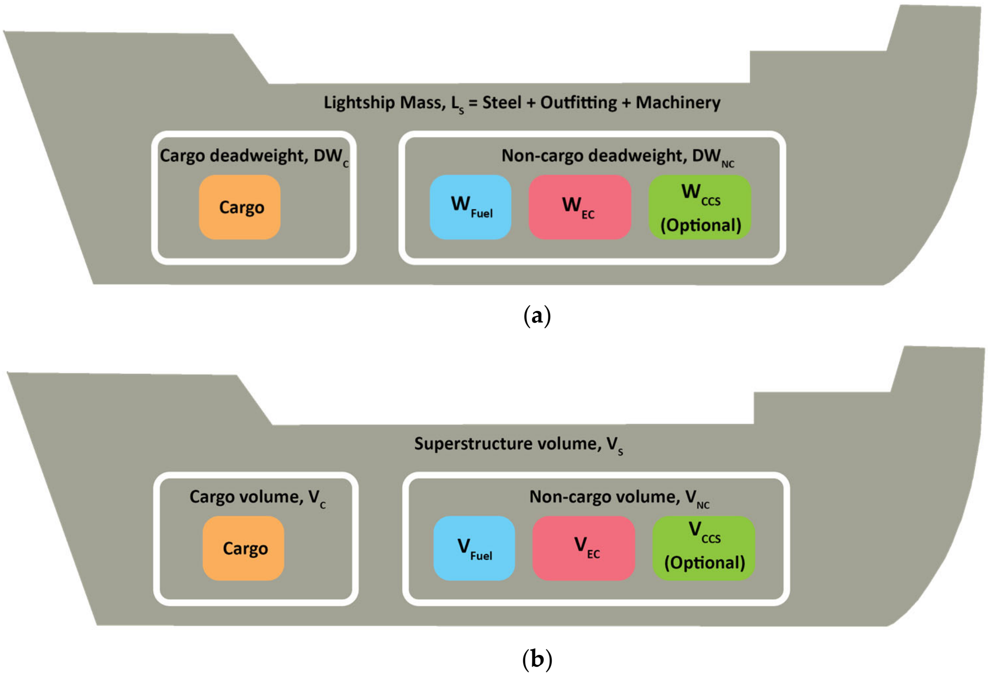

Figure 2. (**a**) Weight and (**b**) volume distributions of a ship.

The weight and volume distribution of a vessel are visualised in Figure 2. The total weight (“displacement”) of a vessel is composed of the L_S, DW_C, and DW_{NC}. whereas the total volume (“GT”) of a vessel is composed of V_S, V_C, and V_{NC}. In the estimation of CAR, the cargo capacity (i.e., V_C or DW_C) for a vessel powered by alternative fuels was compared to that of the reference ship. The V_C and DW_C for alternative fuels (denoted as $V_{C(AF)}$ and $DW_{C(AF)}$) are calculated from the V_C and DW_C of the reference ship (denoted as $V_{C(RF)}$ and $DW_{C(RF)}$). The details of this calculation are demonstrated in Appendices B and C. In the calculation, the values of L_S and V_S were assumed constant for the same type of ship powered with different fuels, and the changes in weight and volume components of DW_{NC} and V_{NC} are assumed to directly affect the V_C and DW_C; i.e., an increase of V_{NC} and DW_{NC} will reduce the cargo capacity, whereas a decrease in V_{NC} and DW_{NC} will increase the cargo capacity. The weight and volume of fuel (W_{Fuel} and V_{Fuel}), energy converter (W_{EC} and V_{EC}), and CCS system (W_{CCS} and V_{CCS}) were quantified first, and then the differences (ΔW_{Fuel}, ΔV_{Fuel}, ΔW_{EC}, ΔV_{EC}, ΔW_{CCS}, ΔV_{CCS}) between alternative and reference fuel were calculated. With this information, the difference of non-cargo weight and volume (i.e., ΔV_{NC} and ΔDW_{NC}) between alternative fuel and reference fuel were calculated. The corrected values of $V_{C(AF)}$ and $DW_{C(AF)}$ for alternative fuels were calculated and then the CAR was quantified as the ratio of V_C or DW_C of the alternative fuelled ship to the V_C or DW_C of the HFO ship.

Prior to the calculation of CAR, the ship needs to be defined as weight- or volume-critical vessel by considering the available mass and volume capacity for storage of cargo. For comparisons across fuels, the HFO-fuelled similar ship was used, but for comparisons across ship types, an HFO-fuelled containership accommodating cargo with a mass of up to 149,008 tons or volume up to 142,477 m^3, was used as reference. This ship will be weight-critical if the cargo has density of more than 1046 kg/m^3 or stows at less than 0.96 m^3/ton, and volume-critical if the cargo is lighter than 1046 kg/m^3. For a weight-critical vessel, the CAR can be obtained as the ratio of cargo deadweight, as shown by Equation (1). The CAR for a volume-limiting vessel is the ratio of cargo volume as shown by Equation (2). Therefore, in this paper, CAR reported for weight-critical vessels will be based on mass, while the CAR reported for volume-critical vessels is based on volume.

$$\text{Cargo attainment rate } (\%) = \frac{DW_{C(AF)}}{DW_{C(RF)}} \times 100\% \quad (1)$$

$$\text{Cargo attainment rate } (\%) = \frac{V_{C(AF)}}{V_{C(RF)}} \times 100\% \quad (2)$$

Apart from the CAR, three other specific performance indicators for energy, economic, and environmental assessments were included: Cs, Es, and CII, defined in Equations (3)–(5).

$$E_S = \frac{\sum \text{TTW Energy (kJ)}}{\text{Voyage distance (nm)} \times \text{DW(dwt)}} \quad (3)$$

$$C_S = \frac{\sum \text{TTW Cost (\$)}}{\text{Voyage distance (nm)} \times \text{DW(dwt)}} \quad (4)$$

$$CII = \frac{\sum \text{TTW } CO_2\text{Emission } (gCO_2)}{\text{Voyage distance (mile)} \times \text{DW(dwt)}} \quad (5)$$

These three specific indicators have taken the voyage distance and ship deadweight into consideration. E_S and C_S are defined as the total TTW energy and total TTW cost divided by voyage distance and DW. The TTW energy has included the total energy required for production of propulsion work and the energy to operate CCS, which were calculated based on the TTW energy consumption factor and CCS energy consumption factor, both expressed as kJ of energy consumed per kJ of propulsion energy in [17]; hence, the total TTW energy can be obtained by multiplying the sum of TTW energy factors with the kJ of propulsion energy. Similarly, the total TTW cost (OPEX and CAPEX) is also calculated based on the TTW cost factors presented in [17] and include TTW energy, fuel, energy converter, storage, and CCS, all expressed in units of cost per kJ of ship propulsion. The Carbon Intensity Indicator (CII), which was introduced by IMO as a measurement of ship's operational efficiency, is used as a rating system for ship carbon emissions, defined as the total TTW carbon emission divided by voyage distance (nm) and ship capacity (DWT) (Equation (5)). The total TTW carbon emission for biofuels used in ICE, hydrogen and ammonia used in fuel cells, and electricity was assumed equal to zero, whereas the fuel with CCS installation has 90% lower carbon emission than HFO and LNG fuel without CCS, which has operational fuel emission factors of 541 g/kWh [34] and 412 g/kWh [34], respectively.

In this study, four ship design factors were studied. These are ship type, fuel type, cargo type, and voyage distance. The first part of the assessment is the basic exploration for these four ship design factors to visualize the impact of variation of these factors on CAR. Among these four factors, there are two numerical factors: voyage distance and cargo type, quantified as stowage factor; the other two factors are: ship type and fuel type. The significance of each selected design parameters is discussed in the following sub-sections.

2.2. Ship Type

The ship types included are containership, tanker, and cargo ship. The ship dimensions, displacement, and total volume of different ships are different even if the DW is the same, with the difference presented in Figure 3. The L, B, and D of the containership were found to be largest, followed by the cargo ship and the tanker. Indirectly, the displacement and GT of a ship also follows the same trend. The cargo deadweight, DW_C, which is illustrated by the column with stripes in the ship displacement chart, is equal for all ship types; hence, the cargo capacity for a mass-critical ship is the same regardless of ship type. However, the difference in ship dimension has caused a difference in GT and NT. Hence, the cargo volume, V_C, for different types of vessels is different. In short, different ships with same DW have same DW_C but different V_C; hence, different ship types would give different CAR when volume is limiting. In the study of CAR for different ships, the comparisons were carried out in two approaches. First, the same ship (an HFO-fuelled containership travelling 10,000 n.m. and carrying cargo with 1.25 m^3/ton) is used as a reference. Second, the same type of ship powered by HFO is also used as a reference, i.e., HFO-fuelled containership, HFO-fuelled tanker, and HFO-fuelled cargo ship are used to calculate the CAR for containership, tanker, and cargo ship powered by alternative fuels, respectively. The first comparison reveals the differences between ships, whereas the second comparison quantifies the impact of fuel transition on CAR for the same ship.

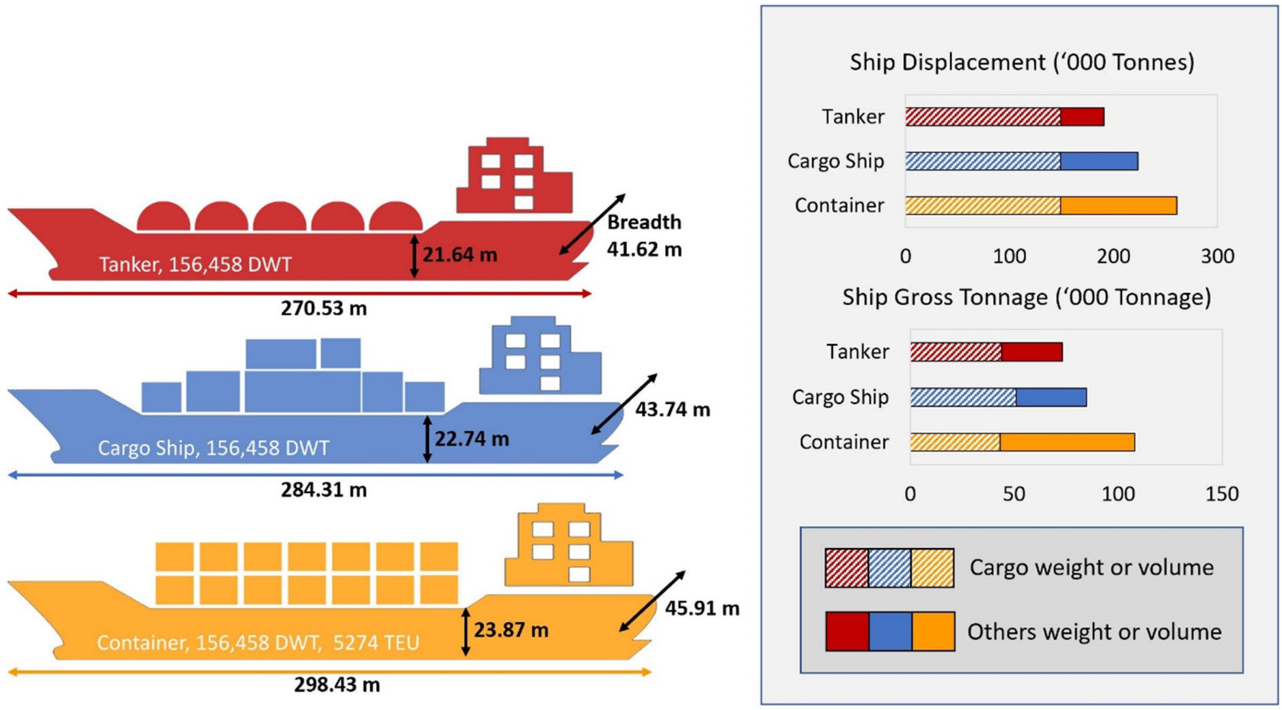

Figure 3. Comparison of the dimension, displacement, and gross tonnage of containership, cargo ship, and tanker with same design deadweight.

2.3. Fuel Type

Eight types of fuels are included with HFO without CCS as the reference, and the seven alternative fuels are: HFO with CCS, LNG with CCS, biodiesel, bio-methanol, and blue fuels produced from natural gas including natural gas-based hydrogen, natural gas-based ammonia, and natural gas-based electricity (denoted as NG-H2, NG-NH3 and NG-E respectively). From the results of comparison between various fuels in terms of fuel mass, fuel volume, lifecycle energy, lifecycle cost, and lifecycle GHG emission presented in [17], the fuel selection has been shown to be an important factor that can affect the ship's economic and fuel storage space requirement. Hence, different types of fuel with different LHV, volumetric density, and propulsion system, which can affect the V_{Fuel} and W_{Fuel} as well as V_{EC} and W_{EC}, are included in this study to visualize the changes in CAR when alternative fuels are used to replace HFO.

2.4. Cargo Type

Different cargoes have different densities and, hence, stowage factors. Figure 4 shows the type of cargo that are typically transported by sea and the usual range of cargo stowage factors. Vessels carrying low-density cargo require larger cargo space and, hence, fuels with high volumetric density (kJ/m^3) have a greater advantage as they compete less with cargo storage. The effect of variation in cargo type on CAR is very significant. For the reference ship described in Table 1, which is weight-limiting when the cargo stowage factor is less than 0.96 m^3/ton, and volume-limiting if the cargo stows at higher than 0.96 m^3/ton, the study of impact of cargo type on CAR can be carried in two different approaches: (i) when a HFO-fuelled containership travelling 10,000 nm and carrying cargo of 1.25 m^3/ton is used as the reference, and (ii) when the HFO-fuelled containership carries the same type of cargo is used as reference of calculation. The first approach allows the visualization of the sensitivity of both cargo type and fuel type on CAR, whereas the second more directly compares ships carrying exactly the same cargo.

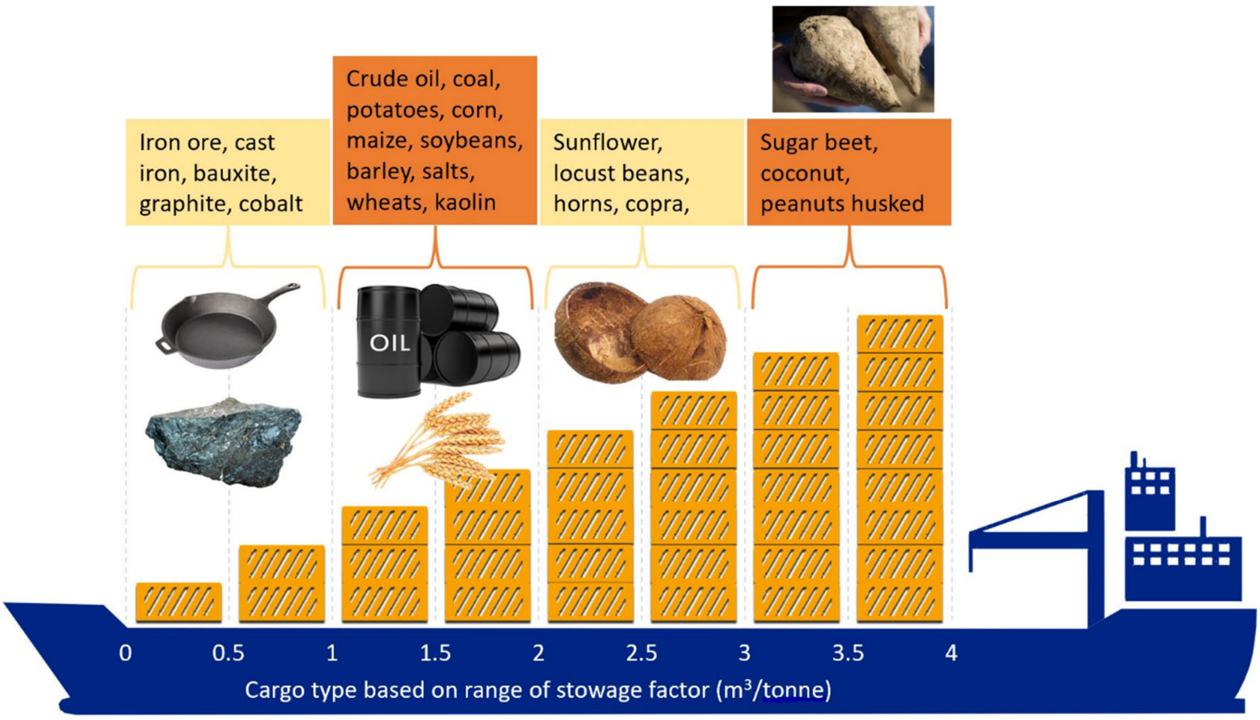

Figure 4. Typical cargos and their stowage factor [26].

2.5. Voyage Distance

The voyage distance has a direct influence on the fuel requirement and hence W_{Fuel} and V_{Fuel} will be affected. A long voyage consumes more fuel, which results in more cargo space loss for onboard storage of fuel. In the study of relationships between voyage distance and CAR for various fuels, two studies were included: (i) when the ship is mass critical carrying cargo with stowage factor of 0.75 m^3/ton, and (ii) when the ship is volume critical carrying cargo with stowage factor of 1.25 m^3/ton. A vessel travelling at 2000–8000 n.m. is here denoted as a short-sea ship, and a vessel travelling distances longer than 8000 n.m. is denoted as a deep-seagoing ship.

2.6. Ship Performance Assessment—Case Studies

After an exploration on the effect of these four design factors on CAR, case studies were carried out so that the performance of various alternative fuels can be compared with the reference to the HFO-fuelled containership. The main goal of the first case study is to determine alternative fuels that are suitable for the deep-seagoing containership travelling an average of 10,000 n.m. per voyage. The performance when powered by different alternative fuels was compared in terms of (i) CAR, (ii) relative E_S, (iii) relative C_S, and (iv) relative CII. In addition, the specific cost to transport a unit mass of cargo per voyage distance was also calculated so that the effect of fuel change can be visualized from different perspectives. In the second case study, operation of the reference ship with different alternative fuels when CAR was limited was between 90% and 100%. When the CAR and cargo loss rate are being fixed, the operation of the ship needs to be adjusted, and here, the manipulating factor is the voyage distance of the vessel.

3. Results

3.1. Quantitative Assessment

3.1.1. Ship Type

CAR versus ship type and fuel type were calculated for both approaches of comparison. The result obtained from the first approach, when the CAR for different type of ships and fuels were calculated based on the same reference ship (HFO-fuelled containership, 10,000 nm, cargo SF of 1.25 m^3/tons) is shown in Figure 5a. It is evident that the CAR for different types of ships is different but it follows a similar trend. Among all ships, the cargo ship has the highest CAR, followed by the containership and the tanker. The CAR of the cargo ship and the tanker are 17.36% and 1.53% higher than the containership, respectively. This difference can be explained by the cargo volume distribution as plotted in Figure 3, where the cargo ship has the highest cargo volume followed by the tanker and the containership. For the second approach, the reference ship HFO-fuelled tanker, HFO-fuelled cargo ship, and HFO-fuelled containership have 100% CAR by definition, and the CAR for the alternative fuels which were calculated based on these reference ships is plotted in Figure 5b. Very small differences between the type of ship are observed. In general, the cargo ship has the highest CAR, followed by the tanker and the containership. For all type of ships discussed, biodiesel gives the highest CAR, followed by bio-MeOH, ammonia, CCS installation, LNG with CCS, hydrogen and, finally electricity. The difference of CAR between various alternative fuels is discussed in more detail in Section 3.1.2.

3.1.2. Fuel Type

The relationship between CAR and fuel type is shown in Figure 5b. For example, the CAR for a containership powered with different alternative fuels as compared to HFO-fuelled containership (10,000 n.m., 1.25 m^3/tons) is shown by the orange-coloured line and markers. All fuels are worse than HFO. The best performing alternative fuel is biodiesel, which reaches more than 99.6% of CAR, whereas Bio-MeOH would result in less than 3% of cargo loss, i.e., higher than 97% CAR. Ammonia and CCS installation for HFO result in slightly more than 3% of cargo loss. LNG with CCS installation and hydrogen would result in more than 4% cargo loss. Among all the alternatives, battery propulsion has the largest cargo loss, so that about 11.8 % of cargo capacity is needed for the storage space requirement for the battery. These trends can be explained by considering the energy per unit volume of each alternative. Because the reference containership with cargo stowed at 1.25 m^3/ton resulted in a volume-critical vessel, fuels with higher volumetric density such as biodiesel require less V_{Fuel} for fuel storage, allowing for more space for carrying cargo. Batteries have the lowest volumetric density among all alternatives (2434 kJ/litre [35]), requiring more V_{Fuel} for energy storage to complete the same journey of 10,000 n.m.

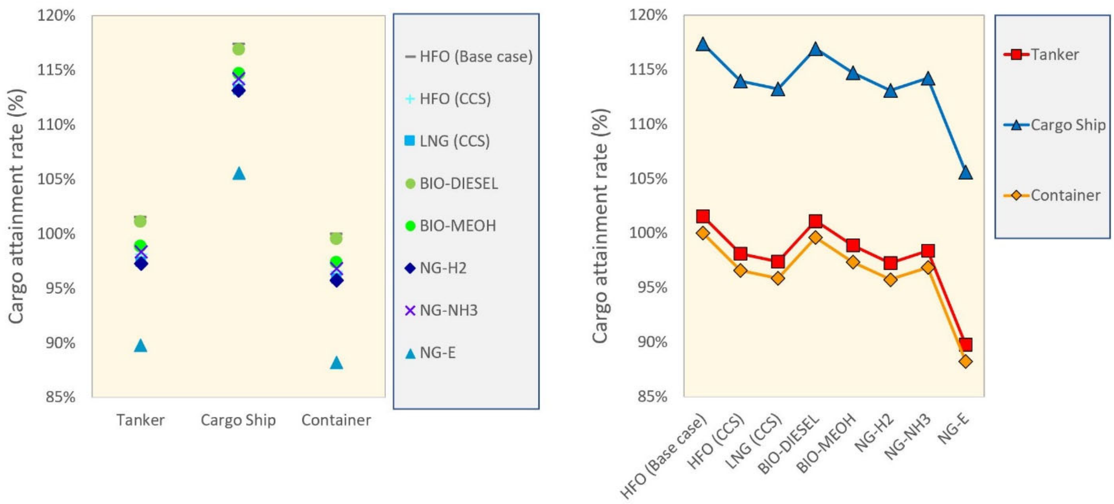

(**a**)

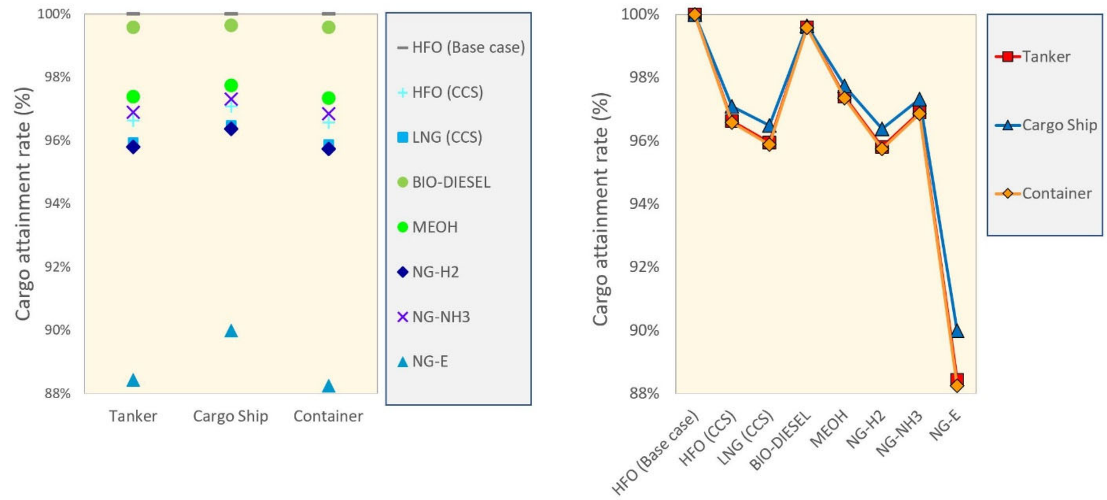

(**b**)

Figure 5. Cargo attainment rate (%) for various ship types and alternative fuels, for a stowage factor of 1.25 m^3/ton and a voyage length of 10,000 nm, (**a**) when the reference ship is HFO-fuelled containership is used, and (**b**) when same type of ship powered by HFO is used as reference ship, i.e., HFO-fuelled containership, HFO-fuelled tanker, and HFO-fuelled cargo ship.

3.1.3. Cargo Type

The CAR for a containership powered by different fuels against cargo stowage factor is shown in Figure 6. The chart is divided into HD and LD zone, which was defined from the total cargo volume and deadweight. The result obtained from first approach is shown in Figure 6a, i.e., the CAR of various fuels is calculated from relative to the same reference ship (HFO-fuelled containership, 10,000 n.m., cargo stowage factor 1.25 m^3/ton). For a ship carrying high-density cargo, for example, SF of 0.75 m^3/ton, the CAR reduced significantly, with the highest CAR of 60.7%, achieved by hydrogen, followed by HFO (60.0%), biodiesel (59.9%), LNG with CCS (59.4%), ammonia (59.3%), bio-MeOH (59.0%), CCS installation for HFO (58.8%) and, finally, electricity (45.5%). The difference of CAR among all fuels expect electricity is minor, whereas electricity gives large reduction (about 15% lower than hydrogen). For cargo stowed at 0.75 m^3/ton, the ship is weight critical. For a weight-critical ship, the cargo storage is limited by DW; hence, fuels with higher LHV give a higher CAR than fuels with lower LHV. This explains why hydrogen (LHV: 120 MJ/kg) shows the highest CAR and the lowest electricity (for battery, LHV: 1.224 MJ/kg [35] and for HFO, LHV: 42 MJ/kg). For a ship carrying low density cargo, for example when SF = 1.25 m^3/ton, the HFO-fuelled containership becomes volume critical. In this case, the reference HFO-fuelled containership has the highest CAR of 100% (by definition), followed by biodiesel (99.6%), bio-MeOH (97.4%), ammonia (96.9%), HFO with CCS (96.6%), LNG with CCS (95.9%) and hydrogen (95.7%) and, lastly, electricity (88.3%). As the cargo stowage factor increases further, the HFO-fuelled containership can carry less compared to a denser cargo due to the CAR, which is now limited by the V_C, and so switching to an alternative fuel can have a proportionally larger reduction in the CAR as the stowage factor increases. Therefore, for example, the conventional HFO ship carrying cargo at 4 m^3/ton has the highest CAR (31.3%), followed by biodiesel (31.1%), bio-MeOH (30.4%), ammonia (30.3%), HFO with CCS (30.2%), LNG with CCS (30.0%) and hydrogen (29.9%) and, lastly, electricity (27.6%).

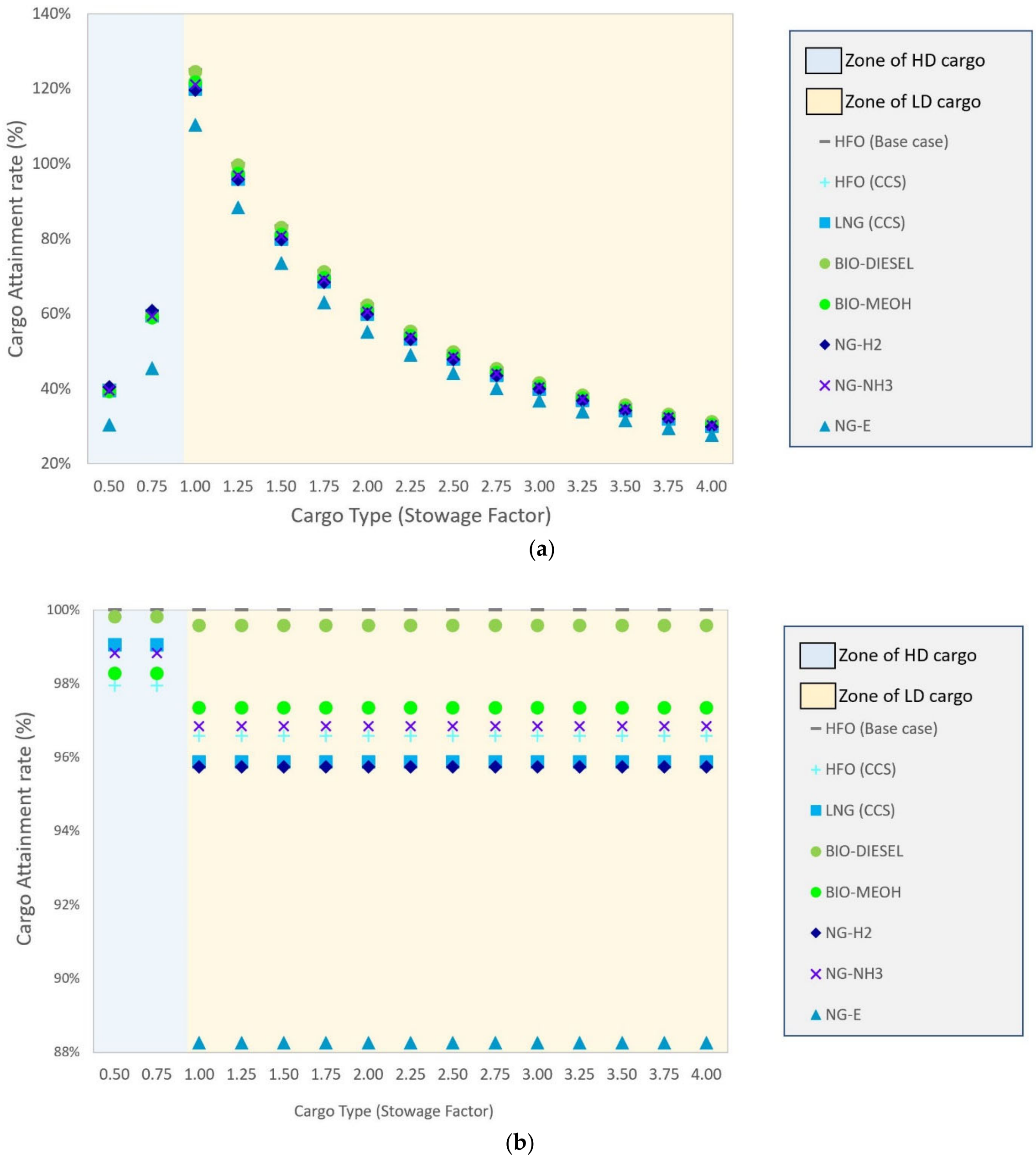

Figure 6. Cargo attainment rate (mass) as a function of cargo stowage factor (m^3/ton) for various fuels, for containership travels a voyage length of 10,000 nm; (**a**) when the reference ship is carrying cargo with SF 1.25 m^3/ton, and (**b**) when the reference ship is carrying the same cargo as the ship being considered.

From the second comparison, when the reference ship is carrying the same type of cargo, the CAR is independent of cargo density. The result obtained is plotted in Figure 6b, which shows that the CAR only varied in two ways. When the ship is weight critical, the CAR for hydrogen is the highest (101.2%), followed by HFO (reference fuel, 100%), biodiesel (99.8%), LNG with CCS (99.1%), ammonia (98.8%), bio-MeOH (98.3%), CCS installation for HFO (98.0%) and, lastly, electricity (75.8%). This order is the same as the weight-critical ship in the first approach, which was discussed above. Secondly, when the ship is volume-critical, as the cargo require a larger storage space, the fuels are ranked again in the same order as the volume-critical ship for the first approach discussed above. Biodiesel has the highest CAR after the reference ship (99.6%), bio-MeOH (97.4%), ammonia (96.9%), HFO with CCS (96.6%), LNG with CCS (95.9%) and hydrogen (95.7%) and, lastly, electricity (88.3%).

The two approaches give different results due to the reference used in the calculation of CAR. In the first approach, comparison was made between ships with different cargo type and, hence, the difference in cargo density also contributed to the difference in CAR; however, the second approach compares the ship carrying the same cargo, hence the CAR is independent of the cargo density.

3.1.4. Voyage Distance

Figure 7 shows the relationship between attainment rate and voyage distance for various type of fuel. The density of the cargo is critical to the performance of the different low-carbon alternatives. The result obtained from the study of a mass-critical ship (0.75 m^3/ton) travelling between 2000 nm to 20,000 nm is plotted in Figure 7a. It is evident that for short-sea shipping (for example, the vessel travels 4000 n.m.), the HFO-fuelled containership has 100% CAR (by definition), hydrogen has a slightly higher CAR of 100.56% due to its higher LHV value, followed by biodiesel (99.92%), LNG (CCS) (99.62%), ammonia (99.60%), bio-MeOH (99.31%), HFO with CCS (99.18%) and, finally, electricity (90.41%). Next, for the deep-seagoing vessel (for example, travelling 10,000 n.m.), hydrogen also has the highest CAR (101.22%), followed by HFO (100%, reference ship), biodiesel (99.81%), LNG (CCS) (99.05%), ammonia (98.83%), bio-MeOH (98.28%), HFO (CCS) (97.95%), and electricity (75.81%). Ships with extremely long range (for example, 20,000 n.m.), the ranking is hydrogen first (102.33%), followed by HFO (100%, reference ship), biodiesel (99.81%), LNG (CCS) (98.10%), ammonia (97.54%), bio-MeOH (96.56%), HFO (CCS) (95.90%) and, lastly, electricity (51.49%).

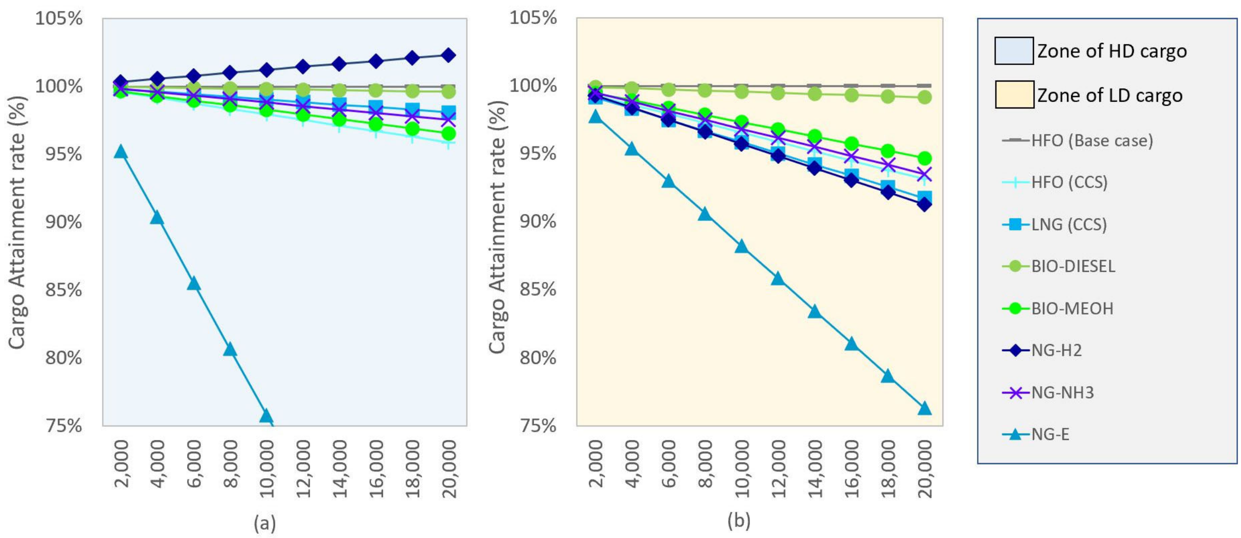

Figure 7. Cargo attainment rate (mass) versus voyage distance (n.m.) for various fuels, for HFO-fuelled containership; (**a**) when the ship is mass critical with SF 0.75 m^3/ton, and (**b**) when the reference ship is volume critical with SF 1.25 m^3/ton.

It is evident that the CAR for various alternative fuels follows the same order, i.e., hydrogen first, followed by the reference fuel HFO and finally electricity, which shows very low CAR compared to the other alternative fuels. The difference in CAR between the alternatives becomes greater with voyage distance, explained by the fact that for trips of longer distance, more fuel needs to be stored onboard and, hence, the increased W_{Fuel} is heavier results in a higher DW_{NC} and, hence, DW_C will be lower which signifies cargo space loss.

In the next part of study, a volume-critical HFO-fuelled containership with a cargo stowage factor of 1.25 m^3/h was used a reference ship. The CAR for all alternative fuels is lower than HFO. For example, when the vessel travels at 10,000 n.m., the CAR is highest for HFO (100%, reference ship), followed by biodiesel (99.6%), bio-MeOH (97.4%), ammonia (96.9%), HFO (CCS) (96.6%), LNG (CCS) (95.9%), hydrogen (95.7%) and, finally, electricity (88.3%). The order of the fuels in terms of CAR is different from the weight-critical vessel because the volume-critical vessel is affected by V_{Fuel} instead of W_{Fuel}. Both weight and volume critical vessels differences in CAR between fuels becomes greater when the voyage distance is longer. HFO with CCS installation gives 98.6%, 96.6%, and 93.2% of CAR when the voyage distance is 4000 n.m., 10,000 n.m., and 20,000 n.m., respectively.

Based on the comparison of the alternative fuel ranking for variation in ship voyage distance, it is concluded that the potential of different fuels to replace HFO as marine fuel onboard a weight-critical vessel and volume-critical vessel are different. The more obvious example is hydrogen; usage of hydrogen for a mass-critical vessel (i.e., dense cargo) is favourable and gives a higher attainment rate than the current HFO. However, application of hydrogen for a volume-critical vessel (i.e., lighter cargo) would result in cargo loss as much as 1.6%, 4.3%, and up to 8.7% compared to the HFO-fuelled containership for voyage distance 4000 n.m.,10,000 n.m., and 20,000 n.m., respectively. The voyage distance can affect the CAR of different fuels differently depending on the cargo type.

3.1.5. Summary

Four factors were investigated above and the effect of variation of these factors towards CAR were discussed in Sections 3.1.1–3.1.4. The percentage changes on cargo attainment rate due to variation of different design factors are summarized in Table 2. Overall, cargo type is the most sensitive factor which would make a ship mass or volume critical and can cause high cargo loss. The next sensitive factor is voyage distance, which has direct impact on the fuel needed; hence, the CAR also changed significantly with voyage distance. Importantly, the type of cargo will make a ship either weight- or volume-critical, altering the sensitivity to distance significantly. Next, the type of marine fuel, which is the key design factor in our study, also greatly changed the CAR; for most cases, all alternatives result in cargo loss, except for dense cargos where H_2 becomes better than HFO. Finally, the ship type seems to be least sensitive factor in estimating the CAR.

Table 2. The range of cargo attainment rate relative to an HFO-fuelled containership without CCS carrying cargo with a stowage factor of 1.25 m^3/ton.

Design Factors	Variation Range	Range of Cargo Attainment Rate (min/max)
Ship type	Three ship types: tanker, cargo ship, containership	0%/1.74%
Fuel type	Eight fuel types: HFO (no CCS), HFO (CCS), LNG (CCS), bio-diesel, bio-MeOH, H_2, NH_3, electricity	0%/−11.75%
Cargo type: stowage factor (m^3/ton)	0.5 m^3/ton–4 m^3/ton	25.00%/−72.42%
Voyage distance (n.m.)	2,000 n.m.–20,000 n.m.	2.33%/−48.51%

3.2. Case Study 1: Economic Cost and Carbon Indices for a Given Cargo and Voyage Length

In this Section, the comparison of the various alternative fuels is extended to include cost and carbon footprint. The comparison is done against a deep-seagoing HFO-fuelled containership, stowage factor 1.25 m^3/ton, and voyage distance of 10,000 n.m. Figure 8 shows the CAR of the various alternatives with the relative values of E_S, C_S, and CII included as points in the same figure. For this case, in terms of CAR, biodiesel is the best (99.6%), followed by bio-MeOH (97.4%), ammonia (96.9%), HFO (CCS) (96.6%), LNG (CCS) (95.9%), hydrogen (95.7%) and, finally, electricity (88.3%). As a way to visualize how the CAR on its own can help take policy or investment decisions, let us assume that 3% cargo loss is acceptable, justified as the cost due to reduced cargo being relatively small compared to fuel price and capital cost, which account for more than 90% of the annualized cost of vessel operation [21]. Among all, biodiesel and bio-MeOH can replace HFO with less than 3% of cargo loss. However, ammonia, HFO with CCS, LNG with CCS, hydrogen, and electricity are not able to meet the 3% of cargo loss limit.

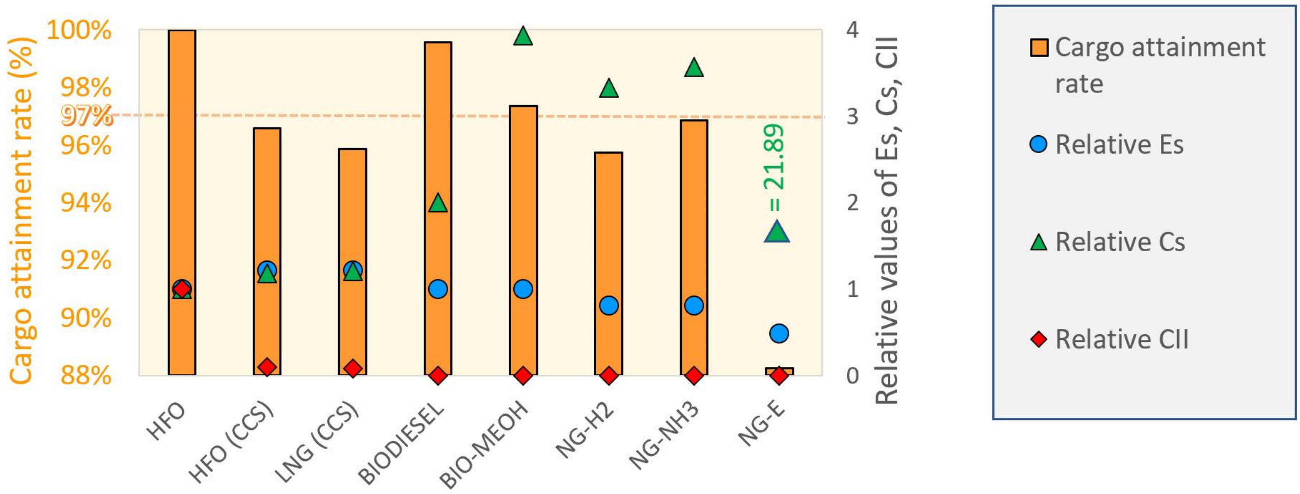

Figure 8. Cargo attainment rate (clustered columns) and relative values of Tank-To-Wake energy unit weight and distance, E_S, economic cost (including fuel cost) per unit weight and distance C_S, and carbon intensity index (gCO_2 per unit weight and distance, CII (scatter points). The reference is an HFO-fuelled containership carrying 1.25 m^3/ton for 10,000 nm.

In terms of E_S, i.e., the Tank-To-Wake energy needed per unit weight and distance travelled, the reference HFO-fuelled containership has an E_S value equal to 55.92 kJ/dwt.nm. The other fuels are normalized to this value to give the relative E_S, shown in Figure 8. HFO with CCS and LNG with CCS are 22% higher due to the additional energy required for operation of CCS, whereas the E_S for biodiesel and bio-MeOH are equivalent to HFO. The other alternatives including electricity (0.49), ammonia (0.81), and hydrogen (0.81) have a lower relative E_S due to the higher efficiency of FC and EM during energy conversion. On a lifecycle basis of course [17], the picture could be different since significant energy is needed to produce these fuels, and the "Well-to-Wake" results from Ref. [17] could be used.

In terms of carbon intensity, the CII value of the reference HFO-fuelled containership was calculated as 3.78 gCO_2/ dwt.nm, consistent with the value of CII presented by DNV [36]. The vessel operated using fuels produced by renewable sources has CII of zero, whereas fossil fuels with CCS installation have CII smaller or equal to 0.38 gCO_2/dwt.nm. Therefore, all alternative fuels are able to achieve at least 90% of carbon reduction.

In terms of Tank-To-Wake economic cost, the C_S of HFO is taken as \$0.00049/dwt.nm. The relative C_S of the alternatives are as follows: HFO with CCS (1.19), LNG with CCS (1.21), biodiesel (2.01), hydrogen (3.33), ammonia (3.57), bio-MeOH (3.94), and electricity (21.89), i.e., all have higher C_S than HFO. Among all, CCS installation is the most cost-effective alternative, which increases the TTW cost by about 20%. The large difference in the C_S of many of the alternatives is mainly attributed to their high price and the higher cost of propulsion system.

We remind that the definition of C_S used above (Equation (4)) is cost per deadweight, not per weight of the cargo only. For a more precise interpretation of vessel economics from an operator's point of view, the cost to deliver a unit mass of cargo must also be quantified and since the amount of cargo delivered may be smaller in order to make extra room for the fuel, the cost per unit cargo increases. Figure 9 shows the estimated freight cost for the different fuels. The reference ship has the lowest freight rate of $5.17 to deliver one ton of cargo to a distance of 10,000 n.m., followed by HFO with CCS ($6.27), LNG with CCS, ($6.30), biodiesel ($10.40), hydrogen ($16.99), ammonia ($18.66), bio-MeOH ($20.71) and, finally, electricity ($149.19). Although these values are based on the current fuel price and technology cost, which may be lowered following technology developments, the relative magnitude is instructive. The potential of alternative fuels also depends on the acceptance of the consumers to pay for the service, as the increment in transportation cost will increase the freight rate, which is to be borne by the consumer.

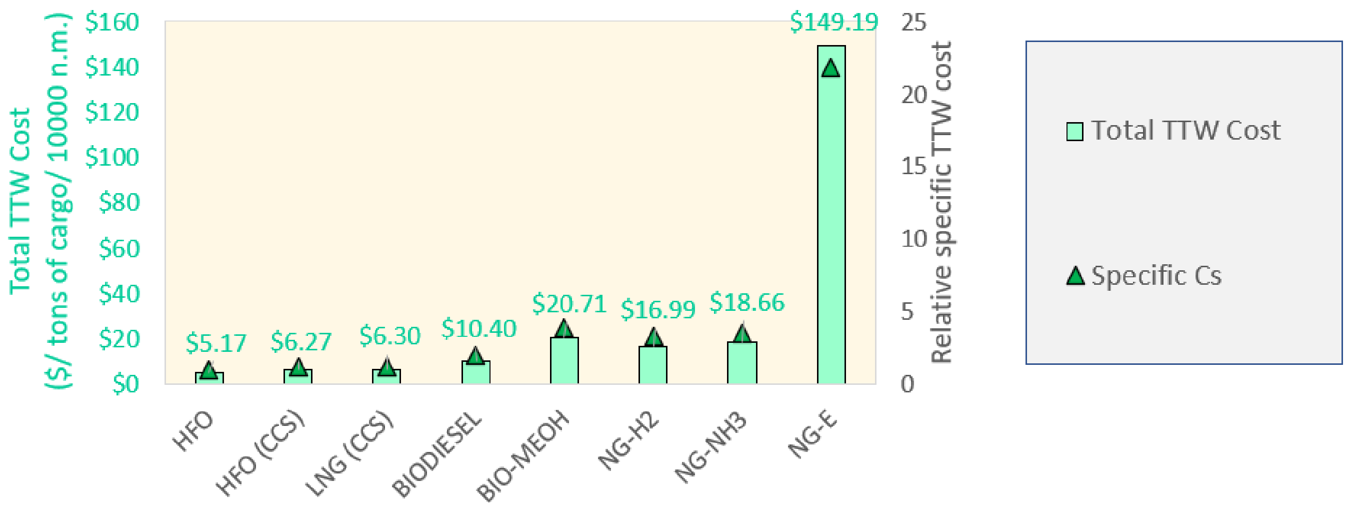

Figure 9. Total cost for transporting 1 ton of cargo for 10,000 nm (columns) and relative C_S (triangles) for the various fuels. The reference is an HFO-fuelled containership carrying 1.25 m^3/ton for 10,000 nm.

To reach a single metric that can be used for comparison across fuels, the normalized CAR, E_S, C_S, and CII can be given a weight and then summed. As an example, here each factor is given an equal weight of 25%. The normalized scores are shown in Figure 10, for the cargo and voyage used in this section. The higher the normalized score, the higher the potential of the fuel to replace HFO as marine fuel. From Figure 10, biodiesel achieves the highest score of 80%, followed by ammonia (79%), hydrogen (77%), bio-MeOH (73%), HFO with CCS (65%), LNG with CCS (64%), HFO (58%) and, finally, electricity (33%). Therefore, giving equal weight to CAR, cost, energy and carbon footprint, biodiesel seems to offer the best compromise, but all other alternative fuels except for electricity are also potential candidates to replace HFO. Different weighting factors may be given by policy-makers or operators to account for their different priorities; the present results can be used as inputs to give overall rankings based on the user's choices.

3.3. Case Study 2: Performance of Alternative Fuels as a Function of Voyage Length

In this section, the example of the HFO containership carrying a cargo with stowage factor 1.25 m^3/ton is used again, but now the voyage distance is a parameter. Figure 11 shows the CAR as a function of distance. If 3% cargo loss is considered acceptable, the zone between 97% to 100% CAR is taken as a possible region for a future fuel and is coloured in green for the purpose of visualization. It is evident that all alternative fuels could be utilized for propulsion of containership within the desired CAR but with limited voyage distance. For example, all fuels can achieve 100% CAR, but the HFO ship can travel the longest voyage distance (10,000 n.m.), followed by biodiesel (7920 n.m.), bio-MeOH (3929 n.m.), ammonia (3435 n.m.), HFO with CCS (3310 n.m.), LNG with CCS (2731 n.m.), hydrogen (2727 n.m.), and electricity (1313 n.m.). If 3% of cargo loss is allowed, biodiesel, bio-MeOH, and ammonia can travel distances longer than 10,000 n.m., and vessels powered by HFO with CCS, LNG with CCS, hydrogen, and electricity can travel up to 9096 n.m., 7922 n.m., 7866 n.m., and 3316 n.m., respectively.

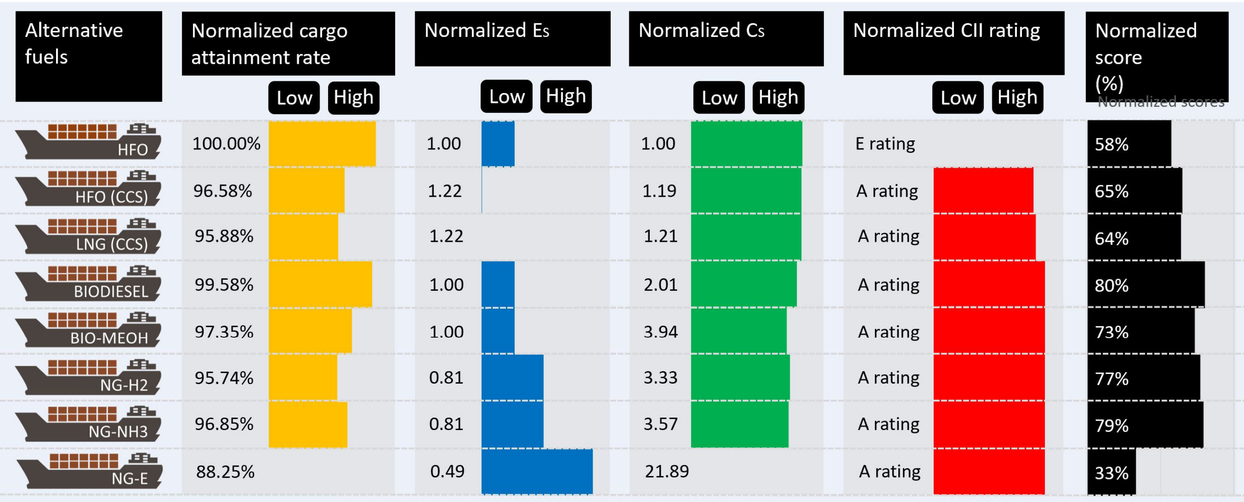

Figure 10. Normalised performance factors for a cargo of 1.25 m^3/ton transported for 10,000 nm and overall score, assuming equal weighting of the four factors (cargo attainment rate, specific energy, specific cost, and CII).

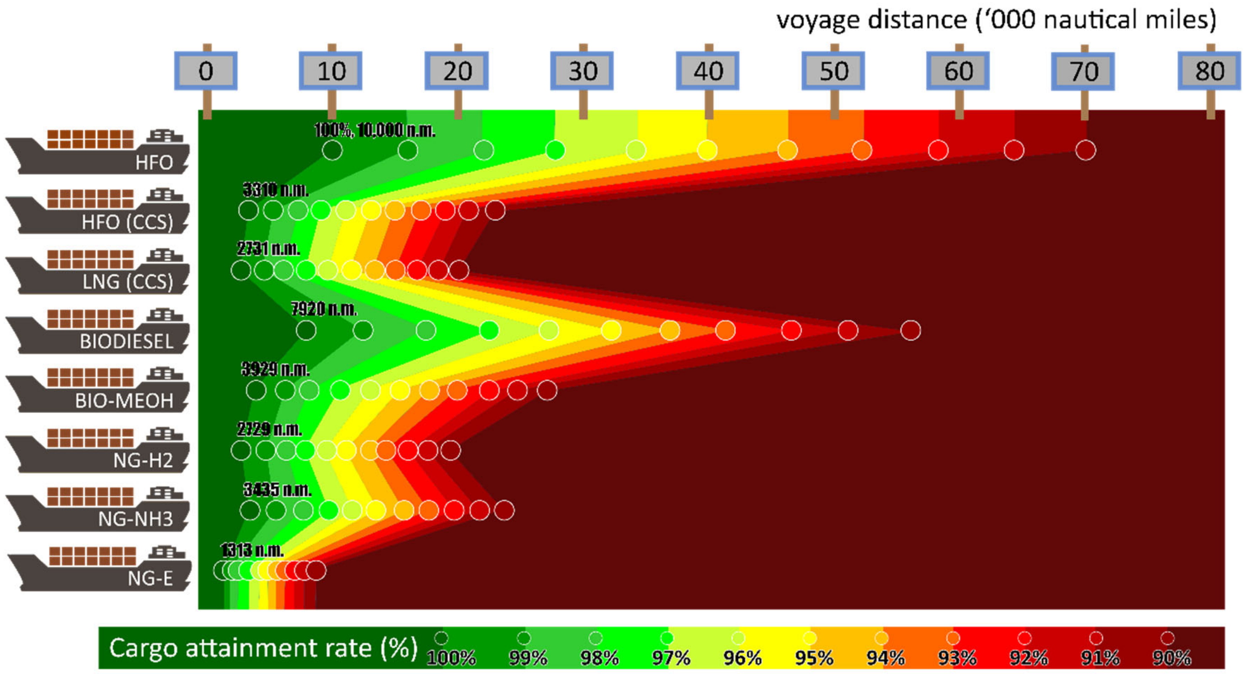

Figure 11. Cargo attainment rate for various alternative fuels against voyage distance, for ships carrying 1.25 m^3/ton. The reference is an HFO-fuelled containership carrying 1.25 m^3/ton for 10,000 nm.

Figure 12 shows a scenario-based analysis for containership with a voyage distance of 10,000 nm. Scenario 1 provides the cargo attainment percentage achievable when voyage distance is fixed at 10,000 nm, Scenario 2 provides the frequency of refuelling required so that the vessel can travel 10,000 n.m. with 100% CAR, and Scenario 3 provides the frequency of refuelling required to travel 10,000 n.m. when 3% cargo loss is acceptable. From the results of Scenario 2, presented in Figure 12, for completion of a journey of 10,000 nm without cargo loss, all alternative fuels need to carry out bunkering in the middle of voyage with battery vessels needing the highest frequency of bunkering. From Scenario 3, the ship with LNG with CCS and the hydrogen ship can reach 10,000 n.m. with one refuelling, whereas battery vessels can travel 10,000 nm with two-time refuelling.

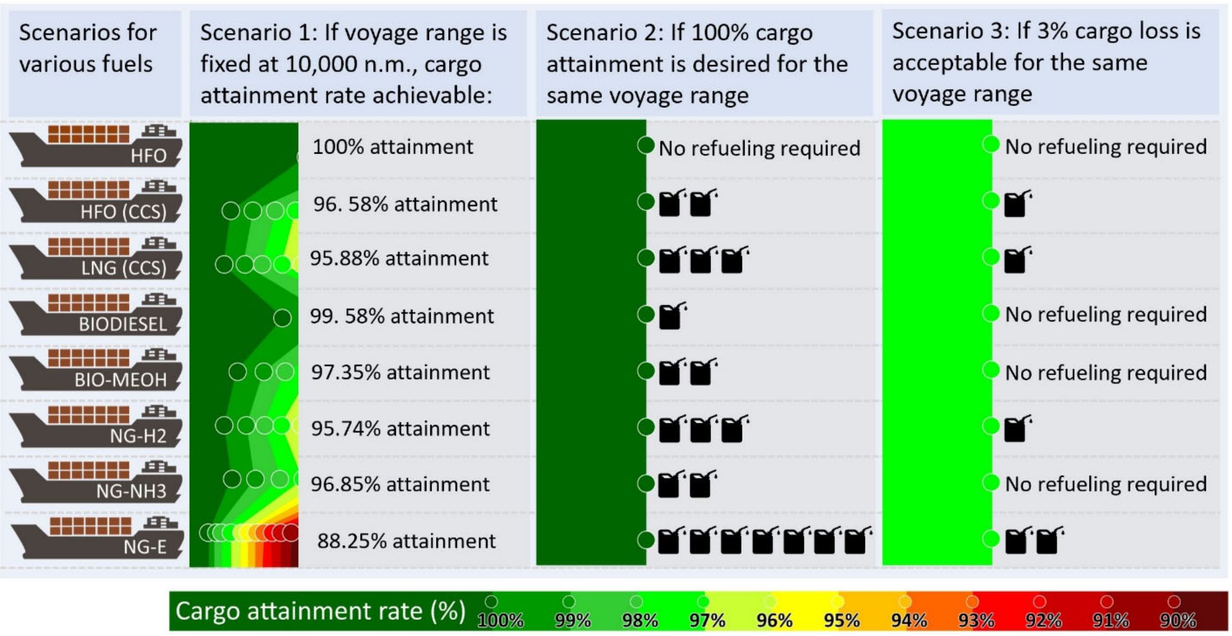

Figure 12. Scenarios-based analysis for deep-seagoing containership with voyage distance of 10,000 nm.

4. Discussion

From a Well-to-Wake perspective, the results of Ref. [17] compared 22 different pathways of primary energy source, fuels, and propulsion systems. The comparison was made on the basis of work at the propeller, i.e., how much energy is needed and how much carbon is emitted on a lifecycle basis to deliver a given amount of work. However, more refined data may be needed by policy makers and ship operators to decide routes and decarbonization strategies, and such an effort was presented in this paper. Seven alternative fuels have been selected regardless of the primary energy source and the analysis was done from a Tank-to-Wake perspective. The present results demonstrate that cargo must be displaced to account for the alternative fuel and its propulsion system, and each decarbonization alternative will come with a range of energy and economic penalties depending on the cargo stowage factor and voyage length. In addition, performance indices must be carefully defined: for instance, should they be per deadweight or per cargo weight? Here, the CAR and the relative $E_{S,}$ C_S, and CII were obtained for a range of ship types and alternative fuels.

The effect of ship type, cargo type (stowage factor), voyage length, and fuel type on CAR are summarized in Table 2. The conclusion is that cargo type, fuel type, and voyage distance are significant design factors in determining ship performance, while the ship type has shown minor impact on CAR. Detailed estimates of CAR as a function of fuel type, ship type, stowage factor, and voyage length are shown in Figures 5–7. In this research, cargo type is represented by the stowage factor (m^3/ton), and here CAR was calculated by reference to a given HFO ship (type, stowage factor, distance travelled) or by referring to the same ship with the same cargo type but burning HFO. The first type of comparison assists sector-wide estimates, while the latter is helpful for assessments of individual ship operations. The CAR of alternative fuels depends on whether the cargo is high-density or low-density. A high-density cargo makes a ship weight critical, and then a fuel with high LHV, such as hydrogen, gives the highest CAR. In contrast, a volume-critical ship has the highest CAR with a fuel of high volumetric density. Importantly, the definition of high- or low-density cargo depends on the available V_C and DW_C of a ship, which was discussed in Section 2.1. Next, voyage distance is closely related to the quantity of fuel needed to complete the voyage. In general, a longer voyage is accompanied by a lower CAR due to the larger W_{Fuel} and V_{Fuel}. However, there is an exceptional case for a weight-critical ship powered by hydrogen, which has a higher LHV value than the reference HFO fuel. Different fuel types result in variation in CAR due to the differences in weight and volume of fuel (W_{Fuel} and V_{Fuel}) and energy converter (W_{EC} and V_{EC}), as well as the additional weight and volume of the CCS system (W_{CCS} and V_{CCS}). The ship type yields only minor differences in CAR, suggesting that decarbonisation solutions would have similar effectiveness across all ships.

Next, two examples were analysed to compare the performance of various alternative fuels for a deep-seagoing containership with cargo stows at 1.25 m^3/ton. The various indices were given equal weight in an effort to provide a single metric. The performance of various fuels for both case studies was compared against the reference HFO-fuelled containership described in Table 1. From the first case study, the CAR, relative E_S, relative C_S, relative CII, and transportation cost of a unit of cargo for 10,000 n.m. for various fuels are compared, and the results are summarized in Figures 8 and 9. It was found that biodiesel offers the most potential as alternative fuel, followed by ammonia, hydrogen, bio-MeOH, HFO with CCS, and LNG with CCS, and electricity has the lowest potential based on its low CAR and exceptionally high C_S (mostly due to the capital cost of the batteries). More R&D is required to improve the energy density of the batteries so that longer distances can be achieved, and less cargo displaced. However, electricity can still be a potential alternative marine fuel for short-sea shipping, suggested by the increasing number of hybrid and electrical-propulsion vessels over the years.

Case study 2 was then carried out to study the feasibility to use all types of alternative fuels, especially electricity for ships. The case study showed that all alternatives can replace HFO as marine fuel including electricity, but with a shorter voyage distance if we are to ensure that a 3% cargo loss limit is not exceeded (assuming this is a reasonable value for acceptable cargo loss). Refuelling can also be planned to extend the voyage distance of the vessel.

The results in Section 3.1 are independent of policy priorities and are based only on estimates of propulsion system efficiencies, fuel cost, and ship design methodologies. Therefore, the evaluation of the various performance indices (CAR, C_S, E_S, and CII) is relatively robust. The results in Sections 3.2 and 3.3 depend on the weighting factors given to the various indices, which depend on the stakeholder's priorities. Here, an equal weight is given as an example, but obviously the ranking between decarbonization options can be different if priorities are different. The present results and modelling can assist with the corresponding quantitative estimates.

5. Conclusions

This study carried out a fleet-level assessment to determine the suitability of seven selected alternative fuels to replace HFO as marine fuel. The fleet-level assessment was started by building a model based on empirical design rules with four selected design factors, namely ship type, cargo type, fuel type, and voyage distance. The exploration of these design factors gave the variation of CAR and is summarized in Table 2 with the individual results presented in Figures 5–7. In short, cargo type is the most sensitive factor and determines if a ship is weight- or volume-critical, followed by voyage distance, fuel type and, lastly, ship type, which is the least sensitive factor in terms of CAR. Whether a ship is weight- or volume-critical affects the amount of cargo that must be replaced to allow for the different mass and volumetric densities of the low-carbon fuel and propulsion system. For very dense cargos, hydrogen offers the best performance, but for the usual values of the stowage factor, all fuels perform worse than the current HFO, suggesting decarbonization will come at a severe cost.

Three additional performance indicators, i.e., specific energy E_S, specific cost C_S, and the CII rating for various fuels were calculated. For a reference HFO ship and operation, the E_S, C_S, and CII are 55.92 kJ/dwt.nm, \$0.00049/dwt.nm, and 3.78 gCO_2/dwt.nm, respectively. Each alternative, when compared to the conventional HFO reference ship, ranks differently for each of these indices, and the relative values of these indices showed that fossil fuels with CCS lead to about 90% CII reduction with about 20–30% economic and energy penalty, while the other alternatives reach zero TTW CII but with Cs greater than 3. The individual indices can be combined into one by selection of appropriate weightings, reflecting the user's priorities. If equal weighting is given in each of these indices, then a normalized scoring system can be formed, as shown in Figure 10. Biodiesel has the highest normalized score (80%), followed by ammonia, hydrogen, bio-MeOH, HFO (CCS), LNG (CCS), and finally electricity, with 33%. Further, considering voyage distance and refuelling, the CAR of various alternative fuels were studied, and it was shown that the various decarbonisation alternatives could potentially achieve any desired CAR via voyage planning and adjustment on voyage distance.

In summary, all alternative fuels have potential for decarbonization of the shipping industry but give very different performance as a function of cargo density and voyage distance. The present results can help an operator define an optimal decarbonisation strategy depending on their requirements (their fleet, cargo types, and voyage lengths) and priorities (carbon emission vs. fuel cost).

Author Contributions: Conceptualization, L.C.L., E.M. and S.E.; methodology, L.C.L.; software, L.C.L.; validation, L.C.L. and E.M.; formal analysis, L.C.L.; investigation, L.C.L., E.M. and S.E.; resources, L.C.L. and E.M.; data curation, L.C.L.; writing—original draft preparation, L.C.L.; writing—review and editing, L.C.L., E.M. and S.E.; visualization, L.C.L. and E.M.; supervision, E.M., and S.E.; project administration, L.C.L., E.M. and S.E.; funding acquisition, E.M. and S.E. All authors have read and agreed to the published version of the manuscript.

Funding: This research is supported by the National Research Foundation (NRF), Prime Minister's Office, Singapore, under its Campus for Research Excellence and Technological Enterprise (CREATE) programme.

Conflicts of Interest: The authors declare no conflict of interest. The funders had no role in the design of the study; in the collection, analyses, or interpretation of data; in the writing of the manuscript, or in the decision to publish the results.

Nomenclature

AF	Alternative fuel
B	Ship breadth
CAR	Cargo attainment rate
CCS	Carbon capture and storage
CII	Carbon intensity indicator (gCO_2/dwt.nm)
CO_2e	Carbon dioxide equivalent
C_S	Specific TTW cost, (\$/dwt.nm)
Δ	Ship displacement
DW	Deadweight
DW_C	Cargo deadweight
DW_{NC}	Non-cargo deadweight
DWT	Deadweight tonnage

E_S	Specific TTW energy, (kJ/dwt.nm)
EM	Electrical motor
FC	Fuel cell
GHG	Greenhouse gases
GT	Gross tonnage
H_2	Hydrogen
HD	High density zone
HFO	Heavy fuel oil
ICE	Internal combustion engine
IMO	International Maritime Organization
L	Ship length
LD	Low-density zone
LNG	Liquefied natural gas
LPG	Liquefied petroleum gas
L_S	Lightship mass
MEOH	Methanol
NH_3	Ammonia
NT	Net tonnage
PEM	Proton Exchange Membrane
RF	Reference fuel
SF	Stowage factor
T	Ship draught
TTW	Tank-to-wake
V_C	Cargo volume
V_{CCS}	CCS volume
V_{EC}	Energy converter volume
V_{Fuel}	Fuel volume
V_{NC}	Non-cargo volume
V_S	Superstructure volume
W_{CCS}	CCS weight
W_{EC}	Energy converter weight
W_{Fuel}	Fuel weight

Appendix A Ship Model

A ship model was built for three types of vessels: a tanker, cargo ship, and container-ship using the method of correlation. The basis of calculation was the DW of the ship, which was assumed to be same for different types of ship, with a value of 156,458 DWT. Using the ship's DW and deadweight coefficient (C_D), ship Δ was calculated using Equation (A1). The calculated Δ, which is different for different types of ships, was then applied in Equation (A2) to obtain the ship length, L. From Equation (A3), block coefficient, C_B, is a function of ship length and speed. Ship dimensions: L, B, T, and D were calculated by using the general ratios of the ships (Equations (A4)–(A6)).

$$\Delta = \frac{DW}{C_D} \tag{A1}$$

$$\Delta = 1.025 \times L \times B \times T \times C_B \tag{A2}$$

$$C_B = a - \frac{(b \times V)}{\sqrt{L}};\ a = 1.23,\ b = 0.395 \tag{A3}$$

The general ratio of ship was taken from the Maritime Engineering Handbook [37]:

$$\frac{L}{B} = 6.5 \tag{A4}$$

$$\frac{B}{T} = 2.25 \tag{A5}$$

$$\frac{L}{D} = 12.5 \tag{A6}$$

The L was first assumed, and lastly goal seek function was used to determine L. The difference in displacement for different ship types resulted in a variation of ship dimensions for the tanker, cargo ship, and containership.

Ship Type	Cargo Ship	Tanker	Containership
Deadweight coefficient, C_D	0.7	0.82	0.6

Appendix B Weight Distribution Onboard of Ship

The weight distribution onboard the ship is presented in Figure 2a. In general, the total weight of a vessel, which is also known as displacement, can be defined using Equations (A7) and (A8). The non-cargo deadweight is approximated to be equal to 5% of cargo deadweight [33]. By applying this relationship, DW_C and DW_{NC} were calculated, and these calculated DW_C and DW_{NC} only representing ships that are powered by HFO as the general Equations from (A1)–(A8) were obtained based on existing ship data; hence, corrections need to be included for ships powered by different alternative fuels.

$$\Delta = L_S + DW \tag{A7}$$

$$DW = DW_C + DW_{NC} = 1.05 \times DW_C \tag{A8}$$

$$DW_{NC} = W_{Fuel} + W_{EC} + W_{CCS} \tag{A9}$$

For ships powered by alternative fuels, the DW_{NC} is the sum of fuel W_{Fuel}, W_{EC}, and W_{CCS} (Equation (A9)). In this paper, it is assumed that any changes in non-cargo deadweight or volume, will directly affect the cargo deadweight and volume, whereas the L_S and V_S are assumed to be constant for all types of fuel. To calculate the DW_C and DW_{NC} of alternative fuel, all the weight components of DW_{NC} (Equation (A9)) need to be quantified. Firstly, the specific fuel consumption rate (SFCR) of fuel needs to be calculated by using LHV value of fuel with the consideration of the efficiency of the energy converter (ε) (Equation (A10)). In general, the efficiency of ICE, FC, and EM are equal to 45%, 55.5%, and 92.5%, respectively. By using the SFCR and the rated power of the vessel, the daily fuel consumption rate (DFCR) of the particular vessel can be obtained (Equation (A11)). A total of 10% margin was included to ensure that the fuel available onboard is sufficient to power the ship for the entire journey. Next, the fuel consumption for the complete voyage (VFCR) can be calculated with Equation (A12). The voyage period was obtained based on voyage speed and distance of the reference ship of 14 knots and 10,000 n.m. (Equation (A13)).

$$SFCR\left(\frac{kg\ fuel}{kWh\ propulsion\ energy}\right) = \frac{1}{LHV \times \varepsilon} \tag{A10}$$

$$DFCR\left(\frac{tons\ of\ fuel\ consumed}{day}\right) = \frac{P \times SFCR \times 24}{1000} \times 110\% \tag{A11}$$

$$VFCR\left(\frac{tons\ of\ LNG\ consumed}{voyage}\right) = DFCR \times voyage\ period \tag{A12}$$

$$Voyage\ period\ (day) = \frac{voyage\ distance\ (n.m.)}{voyage\ speed\ (knots)} \times \frac{day}{24\ h} \tag{A13}$$

The next component of DW_{NC} is the W_{EC}. In this research, three types of energy converters: ICE, FC, and EM were included as the three main propulsion systems for the marine industry. Database for energy converters was acquired from a vendor datasheet which included important data, for instance: power output, efficiency, weight, and volume of energy converters. The information in (Table A1) is used to determine the weight and volume of energy converters. For example, an HFO-fuelled tanker with a rated power of 15,310 kW, DF Engine W 14L46DF was chosen as the energy converter. For simplicity, LNG, and biofuels also fitted with the same model of energy converter. Hence, HFO (CCS), LNG (CCS), Biodiesel, and Bio-MeOH have equal W_{EC} as HFO, and this made the weight difference of energy converter negligible for all fuel with ICE propulsion system. The last component of DW_{NC} is the W_{CCS}, which was calculated by assuming that Amine absorber CCS with 90% capture rate is installed downstream of the engine to treat the exhaust flue gas [38]. As CO_2 is the by-product from combustion of fuel, hence, the weight of the fuel will get lighter, whereas the weight of CO_2 will increase with the voyage. Hence, the additional weight contributed by storage of CO_2 is assumed equal to the total weight of CO_2 captured minus the weight of HFO fuel for the same voyage journey. After quantifying the W_{Fuel}, W_{EC}, and W_{CCS}, the difference in DW_{NC} can be calculated by using Equation (A14). Lastly, the difference in DW_{NC} is assumed to change DW_C. An increment in DW_{NC} would result in reduction in capacity of DW_C and vice versa.

$$\Delta DW_{NC} = \Delta W_{Fuel} + \Delta W_{EC} + \Delta W_{CCS} \tag{A14}$$

$$\Delta W_{Fuel} = W_{Fuel(AF)} - W_{Fuel(RF)} \tag{A15}$$

$$\Delta W_{EC} = W_{EC(AF)} - W_{EC(RF)} \tag{A16}$$

$$\Delta W_{CCS} = W_{CCS(AF)} - W_{CCS(RF)} \tag{A17}$$

Table A1. Database of energy converters.

Energy Converter Models	Energy Output (kW)	Speed (RPM)	Efficiency (%)	Weights (tons) [a]	Volume (m^3) [b]
DF Engine W 6L46DF [39]	6870	N.A.	45.0%	112.20	146.95
DF Engine W 7L46DF [39]	8015	N.A.	45.0%	129.80	160.41
DF Engine W 8L46DF [39]	9160	N.A.	45.0%	143.00	180.92
DF Engine W 9L46DF [39]	10,305	N.A.	45.0%	160.60	190.10
DF Engine W 12L46DF [39]	13,740	N.A.	45.0%	202.40	275.00
DF Engine W 14L46DF [39]	16,030	N.A.	45.0%	245.30	302.83
DF Engine W 16L46DF [39]	18,320	N.A.	45.0%	258.50	395.69
EM Engine LPMR850 [40]	850	3000	92.5%	1.90	1.37
EM 710K-04-MEBSSWW	8000	872	92.5%	19.03	16.43
EM 710H-04-MEBSSWW	9000	980	92.5%	20.24	17.56
2X100% EM 710K-04-MEBSSWW	16,000	872	92.5%	38.06	32.85
2X100% EM 710H-04-MEBSSWW	18,000	980	92.5%	40.48	35.12
PEMFC & EM Engine LPMR850 [b]	850	3000	55.5%	2.89	1.96
PEMFC & EM 710K-04-MEBSSWW [b]	8000	872	55.5%	28.39	21.93
PEMFC & EM 710H-04-MEBSSWW [b]	9000	980	55.5%	30.77	23.75
PEMFC & 2X100% EM 710K-04-MEBSSWW [b]	16,000	872	55.5%	75.51	54.85
PEMFC & 2X100% EM 710H-04-MEBSSWW [b]	18,000	980	55.5%	82.61	59.87

[a] Weights and volume are added with 10% margin. [b] Fuel cell propulsion system is assumed to be combination of PEM fuel cell model and electrical motor.

The calculation for weight distribution of the reference ship using LNG (CCS) as marine fuel is demonstrated below as an example.

Firstly, $W_{Fuel(LNG)}$ was calculated:

Given the LHV of LNG = 49,840 kJ/kg, a reference vessel travelling at speed of 14 knots for 10,000 n.m.:

$$LHV = \frac{49,840}{3600} = 13.84\frac{kWh}{kg}$$

$$SFCR = \frac{1}{13.84 \times 0.45} \approx 0.16\frac{kWh}{kg\ LNG}$$

$$DFCR = \frac{15,310 \times 0.16 \times 24}{1000} \times 110\% \approx 64.88\ \frac{tons\ of\ fuel\ consumed}{day}$$

$$Voyage\ period\ (day) = \frac{10,000}{14} \times \frac{day}{24\ h} \approx 30\ days$$

$$W_{fuel(LNG)} = VFCR = 64.88 \times 30\ days \approx 1,946\ \frac{tons\ LNG}{voyage}$$

From Table A1, the $W_{EC(LNG)}$ was obtained, which equals to 245.3 tons. Next, $W_{CCS(LNG)}$ was calculated:

Given that the operational fuel emission factor for LNG is 412 g/kWh [34], an Amine-based CCS can capture 90% of the CO_2 emitted from the combustion of LNG:

$$CO_{2\ emission}\left(\frac{tons\ CO_2}{voyage}\right) = \frac{412 \times 15,310kW \times 24h \times 30days}{1000 \times 1000} \approx 4541\ \frac{tons\ CO_2}{voyage}$$

$$W_{CCS(LNG)} = CO_{2\ captured}\left(\frac{tons\ CO_2}{voyage}\right) = 4541\ \frac{tons\ CO_2}{voyage} \times 90\% \approx 4,087\frac{tons\ CO_2}{voyage}$$

Similar steps were repeated for the calculation of the $W_{Fuel(HFO)}$, and $W_{EC(HFO)}$, whereas W_{CCS} equal to zero for reference ship without CCS installation.

$$W_{Fuel(HFO)} \approx 2310\ tons$$

$$W_{EC(HFO)} \approx 245.3\ tons$$

$$W_{CCS(HFO)} = 0\ tons$$

Hence, the change of non-cargo DW for fuel transition from HFO to LNG and CCS installation was calculated below. The DW_{NC} has increased by 1413 tons in overall. This increase of non-cargo DW will result in the reduction of cargo capacity by 1413 tons.

$$\Delta W_{Fuel} = 1946 - 2310 = -364\ tons$$

$$\Delta W_{EC} = 245.3 - 245.3 = 0\ tons$$

$$\Delta W_{CCS} = 4087 - 2310 = 1777\ tons$$

$$\Delta DW_{NC} = 1413\ tons$$

Appendix C Volume Distribution Onboard of Ship

Volume distribution onboard of ship is presented in Figure 2b. The overall internal volume of a vessel is known as GT, whereas NT is the total volume available for cargo. Both GT and NT can be calculated by using Equations (A18) and (A20). The total volume equals to summation of V_S, V_C, and V_{NC} (Equation (A21)); and V_S is assumed equal to 35% of the total volume [37]. By using these equations V_S, V_C, and V_{NC} were calculated.

$$GT = k_1 \times CN = Total\ volume \quad (A18)$$

$$CN = L \times B \times D \quad (A19)$$

$$NT = k_2 \times GT = V_C \quad (A20)$$

$$Total\ volume = GT = V_S + V_C + V_{NC} \tag{A21}$$

$$V_S = 35\% \times GT \tag{A22}$$

$$V_{NC} = V_{Fuel} + V_{EC} + V_{CCS} \tag{A23}$$

Ship Type	Cargo Ship	Tanker	Containership
k_1	0.30	0.30	0.33
k_2	0.60	0.60	0.40

The above equations give the volume distribution of the reference ship, and changes in V_{NC} distribution (V_{Fuel}, V_{EC}, and V_{CCS}) caused by utilization of alternative fuels need to be considered to find out the corrected V_C and V_{NC} for alternative fuels. V_{Fuel} can be obtained from division of VFCR with mass density of fuel (ρ_{Fuel}), V_{EC} can be found from Table A1, and lastly the V_{CCS} being considered in this research is the storage volume for captured CO_2 and hence can be obtained from division of total mass of CO_2 captured with mass density of CO_2 (ρ_{CO_2}).

$$V_{fuel} = VFCR \div \rho_{fuel} \tag{A24}$$

$$V_{CCS} = CO_{2\ captured}\left(\frac{tons\ CO_2}{voyage}\right) \div \rho_{CO_2} \tag{A25}$$

$$\Delta V_{NC} = \Delta V_{fuel} + \Delta V_{EC} + \Delta V_{CCS} \tag{A26}$$

$$\Delta V_{Fuel} = V_{Fuel(AF)} - V_{Fuel(RF)} \tag{A27}$$

$$\Delta V_{energy\ converter} = V_{energy\ converter(AF)} - V_{energy\ converter(RF)} \tag{A28}$$

$$\Delta V_{CCS} = V_{CCS(AF)} - V_{Fuel(RF)} \tag{A29}$$

$$V_{C(AF)} = V_{C(RF)} - \Delta V_{NC} \tag{A30}$$

Appendix D Weight- or Volume-Critical Ship

Based on the calculated cargo deadweight and volume of the ship, the ship can be either weight-critical or volume-critical based on the cargo being carried. By using the reference ship in Table 1 as an example, a containership with C_D value of 0.6:

$$\Delta = \frac{156,458}{0.6} = 260,763.33 \text{ tons}$$

Assume ship length, L equal to 298.43 m:

$$B = \frac{298.43}{6.5} = 45.91 \text{ m}$$

$$T = \frac{45.91}{2.25} = 20.41 \text{ m}$$

$$D = \frac{298.43}{12.5} = 23.87 \text{ m}$$

$$C_B = 1.23 - \frac{(0.395 \times 14)}{\sqrt{298.43}} = 0.91$$

For verification, Equation (A2) is used to calculated ship displacement based on the assumed L and the calculated dimensions using the assumed L:

$$\Delta = 1.025 \times 298.43 \times 45.91 \times 20.41 \times 0.91 = 260,830$$

As the ship displacement calculated using both Equations (A1) and (A2) were nearly equal to each other, the assumed L is acceptable and the ship dimension obtained are used for calculation of cargo deadweight and cargo volume in the following calculations.

Cargo deadweight is calculated from Equation (A8),

$$DW_C = \frac{156,458}{1.05} = 149,007.62 \text{ tons}$$

Cargo volume is calculated from Equation (A20),

$$NT = V_C = 0.40 \times 0.33 \times 298.43 \times 45.91 \times 23.87 = 53,976.44 \; tonnage = 142,476.83 \text{ m}^3$$

From the calculated DW_C and V_C, the ship can carry cargo up to 149,008 tons or 142,477 m^3. Cargo attainment capacity can be limited by weight or volume depending on the stowage factor of cargo. For example, when the cargo is stowed at 0.75 m^3/ton, the ship can carry up to 149,008 tons of cargo, which occupies 149,008 m^3 of the ship space, and this ship does not fully utilize the cargo volume as it is limited by the limit of DW_C. In this case, the ship can be defined as "weight-critical", and the cargo attainment rate for weight-critical ship can be calculated by using Equation (1). On the other hand, if the cargo is stowed at 1.25 m^3/ton, the ship can carry 142,477 m^3 of cargo, with total cargo weight of 113,981 tons, and this ship does not fully utilized the cargo deadweight as it is limited by the limit of V_C. Hence, this ship is known as "volume-critical" as the cargo attainment rate can be calculated using Equation (2) as a function of volume.

References

1. International Maritime Organization. *Fourth IMO Greenhouse Gas Study*; International Maritime Organization: London, UK, 2020.
2. Maritime Knowledge Centre; TNO; TU Delft. *Final Report—Framework CO2 Reduction in Shipping*; TU Delft: Delft, Netherlands, 2017.
3. Adland, R.; Cariou, P.; Wolff, F.-C. Optimal ship speed and the cubic law revisited: Empirical evidence from an oiltanker fleet. *Transp. Res. Part E* **2020**, *140*, 101972. [CrossRef]
4. Berthelsen, F.H.; Nielsen, U.D. Predictions of ships' speed-power relationship at speed intervals below the design speed. *Transp. Res. Part D* **2021**, *99*, 102996. [CrossRef]
5. Singh, B. Liquified Natural Gas (LNG) as Fuel for The Shipping Industry. *Marine Insight*, 8 January 2021. Available online: https://www.marineinsight.com/green-shipping/liquified-natural-gas-lng-as-fuel-for-the-shipping-industry/(accessed on 26 March 2022).
6. Frangoul, A. Maersk Spends $1.4 Billion on Ships That Can Run on 'Carbon Neutral' Methanol. *CNBC*, 24 August 2021. Available online: https://www.cnbc.com/2021/08/24/maersk-spends-1point4-billion-on-ships-that-can-run-on-methanol.html(accessed on 26 March 2022).
7. DNV.GL; ZEM. Grenland Energy. In *DNV GL Handbook for Maritime and Offshore Battery Systems*; DNV.GL: Oslo, Norway, 2016.
8. Biogradlija, A. HySeas III Project to Build Hydrogen-Powered Ferry. *Energy News*, 7 June 2021. Available online: https://energynews.biz/hyseas-iii-project-to-build-hydrogen-powered-ferry/(accessed on 15 April 2022).
9. Sakharkar, A. Energy Observer is Equipped with a New Fuel Cell Developed by Toyota. *Tech Explorist*, 6 February 2020. Available online: https://www.techexplorist.com/energy-observer-equipped-fuel-cell-toyota/29871/(accessed on 15 April 2022).
10. Shell. Shell to Trial First Hydrogen Fuel Cell for Ships in Singapore. *Shell*, 21 April 2021. Available online: https://www.shell.com.sg/media/2021-media-releases/shell-to-trial-first-Hydrogen-fuel-cell-for-ships-in-singapore.html(accessed on 15 April 2022).
11. Marine, S. Towards a Decarbonised Future: Sembcorp Marine, Shell and Penguin International Sign MoU for Hydrogen-powered Vessel. *Sembcorp Marine*, 21 April 2021. Available online: https://www.sembmarine.com/2021/04/21/towards-a-decarbonised-future-sembcorp-marine-shell-and-penguin-international-sign-mou-for-hydrogen-powered-vessel(accessed on 15 April 2022).
12. Prevljak, N.H. Value Maritime to Install World's 1st Onboard CCS Unit on Ship in Operation. *Offshore Energy*, 10 September 2021. Available online: https://www.offshore-energy.biz/value-maritime-to-install-worlds-1st-onboard-ccs-unit-on-ship-in-operation/(accessed on 24 June 2022).
13. Deniz, C.; Zincir, B. Environmental and economical assessment of alternative marine fuels. *J. Clean. Prod.* **2016**, *113*, 438–449. [CrossRef]
14. Hansson, J.; Månsson, S.; Brynolf, S.; Grahn, M. Alternative marine fuels: Prospects based on multi-criteria decision analysis. *Biomass-Bioenergy* **2019**, *126*, 159–173. [CrossRef]
15. DNV.GL. Alternative Fuels: The Options. *DNV*, 9 October 2018. Available online: https://www.dnv.com/expert-story/maritime-impact/alternative-fuels.html(accessed on 26 March 2022).

16. DNV.GL. *Assessment of Selected Alternative Fuels and Technologies*; DNV.GL: Hovik, Norway, 2019.
17. DNVGL. *Alternative Fuels for Containerships*; DNVGL: Hovik, Norway, 2021.
18. Law, L.C.; Foscoli, B.; Mastorakos, E.; Evans, S. A Comparison of Alternative Fuels for Shipping in Terms of Lifecycle Energy and Cost. *Energies* **2021**, *14*, 8502. [CrossRef]
19. Lloyd's Register and UMAS. *Techno-Economic Assessment of Zero-Carbon Fuels*; Lloyd's Register and UMAS: London, UK, 2020.
20. Horvath, S.; Fasihi, M.; Breyer, C. Techno-economic analysis of a decarbonized shipping sector: Technology suggestions for a fleet in 2030 and 2040. *Energy Convers. Manag.* **2018**, *164*, 230–241. [CrossRef]
21. Mao, X.; Rutherford, D.; Osipova, L.; Comer, B. *Refueling Assessment of a Zero-Emission Container Corridor between China and the United States: Could Hydrogen Replace Fossil Fuels?* International Council on Clean Transportation: Washington, DC, USA, 2020.
22. Imhoff, T.B.; Gkantonas, S.; Mastorakos, E. Analysing the Performance of Ammonia Powertrains in the Marine Environment. *Energies* **2021**, *14*, 7447. [CrossRef]
23. Smith, J.R.; Gkantonas, S.; Mastorakos, E. Modelling of boil-off and sloshing relevant to future liquid hydrogen carriers. *Energies* **2022**, *15*, 2046. [CrossRef]
24. Kim, K.; Roh, G.; Kim, W.; Chun, K. A Preliminary Study on an Alternative Ship Propulsion System Fueled by Ammonia: Environmental and Economic Assessments. *J. Mar. Sci. Eng.* **2020**, *8*, 183. [CrossRef]
25. Korberg, A.; Brynolf, S.; Grahn, M.; Skov, I.R. Techno-economic assessment of advanced fuels and propulsion systems in future fossil-free ships. *Renew. Sustain. Energy Rev.* **2021**, *142*, 110861. [CrossRef]
26. ONZE. Stowage Factor. ONZE. Available online: https://www.onze.lt/en/cargo-transport-by-sea/stowage-factor/#:~{}:text=The%20stowage%20factor%20is%20calculated%3A%20one%20large%20ton,load%20one%20long%20tonne%20of%20a%20given%20load (accessed on 10 March 2022).
27. Stolz, B.; Held, M.; Georges, G.; Boulouchos, K. Techno-economic analysis of renewable fuels for ships carrying bulk cargo in Europe. *Nat. Energy* **2022**, *7*, 203–212. [CrossRef]
28. Lloyd's Register. Carbon Intensity Indicator. Lloyd's Register, LR. Available online: https://www.lr.org/en/carbon-intensity-indicator/#:~{}:text=The%20Carbon%20Intensity%20Indicator%20%28CII%29%20is%20a%20rating,above%205%2C000%20gross%20tonnage%20%28GT%29%20and%20trading%20internationally (accessed on 30 May 2022).
29. DNV. CII—Carbon Intensity Indicator. DNV. Available online: https://www.dnv.com/maritime/insights/topics/CII-carbon-intensity-indicator/index.html (accessed on 24 June 2022).
30. Marine Optima. Maean Helen. Marine Optima. Available online: https://app.maritimeoptima.com/vesselcenter/vessels/9779381?tab=public-description (accessed on 1 January 2022).
31. VesselFinder. MARAN HELEN Crude Oil Tanker, IMO 9779381. Available online: https://www.vesselfinder.com/vessels/MARAN-HELEN-IMO-9779381-MMSI-241491000 (accessed on 1 January 2022).
32. Watson, D. *Practical Ship Design*; Elsevier Ocean Engineering Book Series; Elsevier: Amsterdam, The Netherlands; London/Oxford, UK; New York, NY, USA; Shannon, Ireland; Paris, France; Tokyo, Japan, 1998; p. 531.
33. Ventura, M. Estimation Methods for Basic Ship Design. Available online: http://www.mar.ist.utl.pt/mventura/Projecto-Navios-I/EN/SD-1.3.1-Estimation%20Methods.pdf (accessed on 5 April 2022).
34. Gilbert, P.; Walsh, C.; Traut, M.; Kesieme, U.; Pazouki, K.; Murphy, A. Assessment of full life-cycle air emissions of alternative shipping fuels. *J. Clean. Prod.* **2018**, *172*, 855–866. [CrossRef]
35. Wua, P.; Bucknalla, R. Marine propulsion using battery power. In Proceedings of the Shipping in Changing Climates Conference 2016, London, UK, 10–11 November 2016.
36. DNV. *The Carbon Intensity Indicator (CII)—A Closer Look*; DNV: Høvik, Norway, 2021.
37. Molland, A.F. *The Maritime Engineering Reference Book—A Guide to Ship Design*; Elsevier: Alpharetta, GA, USA, 2008.
38. Law, L.C.; Azudin, N.Y.; Shukor, S.R.A. Optimisation of Operational Parameter and Economic Analysis of Amine Based Acid Gas Capture Unit. *Chem. Eng. Trans.* **2017**, *56*, 73–78. [CrossRef]
39. Wärtsilä. *Wärtsilä 46D Product Guide*; Wärtsilä Finland: Helsinki, Finland, 2019.
40. Virtualexpo Group. All Tema D.O.O. Products. Available online: https://www.nauticexpo.com/prod/tema-doo-39710.html (accessed on 6 April 2022).